




# Carbon dots-based catalyst for various organic transformations

Ravichandran Manjupriya<sup>1</sup> and Selvaraj Mohana Roopan<sup>1,\*</sup> 

<sup>1</sup>Chemistry of Heterocycles and Natural Product Research Laboratory, Department of Chemistry, School of Advanced Sciences, Vellore Institute of Technology, Vellore, Tamil Nadu 632 014, India

**Received:** 21 April 2021

**Accepted:** 16 July 2021

**Published online:**

22 August 2021

© The Author(s), under exclusive licence to Springer Science+Business Media, LLC, part of Springer Nature 2021

## ABSTRACT

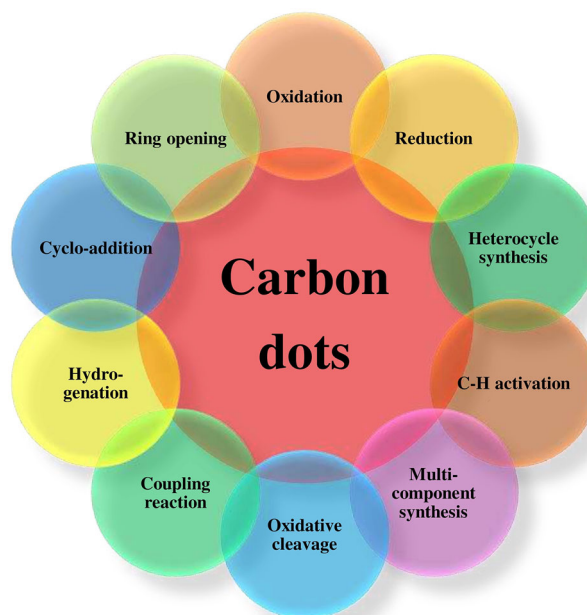
Carbon dots (CDs), owing to their zero-dimensional structure and outstanding physicochemical features, can be used as a support to metals, metal oxides, to form nanocomposites, thus emerging as promising nanocatalysts to drive various organic transformations. For this reason, we planned to review the usage and advantages of these carbon dots and their supported catalysts, in various organic reactions. Furthermore, the recent advancements in CDs to develop it as an amphiphilic catalyst to use an environmentally benign solvent (water) to solvate organic reactants in organic reactions have also been discussed.

Handling Editor: Chris Cornelius.

Address correspondence to E-mail: mohanarooopans@vit.ac.in; mohanarooopans@gmail.com

<https://doi.org/10.1007/s10853-021-06354-7>

## GRAPHICAL ABSTRACT

**Abbreviations**

[APMim][Cl]	1-Aminopropyl-3-methylimidazolium chloride	HPU	Hyperbranched polyurethane
BPEI	Branched polyethyleneimine	IRMOF	Isoreticular metal–organic framework
c-CDs	Carboxyl functionalized carbon dots	IL	Ionic liquid
CDs	Carbon dots	LDH	Layered double hydroxide
CDNS	Cyclodextrin nanosponges	LED	Light-emitting diode
CNDs	Carbon nanodots	MeOH	Methanol
$^{13}\text{C}$ NMR	$^{13}\text{C}$ Nuclear magnetic resonance spectroscopy	MOF	Metal–organic frameworks
CSC	Coconut shell char	n-CDs	Amine-functionalized carbon dots
CA	Citric acid	N-CDs	Nitrogen-doped carbon dots
CQDs	Carbon quantum dots	NPs	Nanoparticles
CRS	Colloidal reaction system	NR	No reaction
DAB	1,4-Diaminobutane	NWs	Nanowires
DDA	Dodecylamine	PB	Prussian blue
EDTA	Ethylenediaminetetraacetic acid	PL	Photoluminescence
FTIR	Fourier-transform infrared spectroscopy	PVP	Poly-(N-vinyl-2-pyrrolidone)
g-C <sub>3</sub> N <sub>4</sub>	Graphitic carbon nitride	QY	Quantum yield
GO	Graphene oxide	r-CDs	Reduced carbon dots
GQDs	Graphene quantum dots	TBHP	Tertiary butyl hydroperoxide
		TGA	Thermogravimetric analysis
		TEOA	Triethanolamine
		TEM	Transmission electron microscopy
		THF	Tetrahydrofuran
		TOF	Turnover frequency

TON	Turnover number
UV–Vis	Ultraviolet–visible spectroscopy
XRD	X-ray diffraction
XPS	X-ray photoelectron spectroscopy

## Introduction

Carbon dots (CDs) are fluorescent, carbon-based zero-dimensional materials comprising quasi-spherical nanoparticles [1] usually in size less than 10 nm in range. These CDs are made of  $sp^2/sp^3$  hybridized carbon [2]. Carbon dots can also be designated as carbon nanodots (CNDs) or carbon quantum dots (CQDs) [3]. The word “*quantum*” is referred to as the nanostructures having delocalized band sizes and structures in a quantum-confined regime [4]. Noticeably, CDs coordinate special optical properties of quantum dots with the carbon materials’ electronic properties. It also acquires superior fluorescent properties, includes controllable emission spectra and broad excitation spectra, and possesses excellent photostability against photoblinking and bleaching, distinguishing it from other fluorescent and ordinary semiconductor quantum dots [5, 6]. Due to low cost, ease of synthesis, non-toxicity, good stability, and optical properties, carbon dots are being used in the photocatalytic solar-to-energy conversion, and they usually act as either electron acceptors or donors [7–9]. Also, they can be used to combine with other materials that boost photocatalytic efficiency through distinctive interfacial regions to raise the concentration of available charge carriers for photoreactions and to promote the separation of charges. Such carbon dots can be coupled with semiconductors, metals, molecules, and conjugated compounds with a variety of applications in photocatalytic degradation [10–13], carbon dioxide conversion [14], hydrogen evolution [15–18], bioimaging [5], sensors [19], drug delivery [20], and fine organic synthesis [21].

Among the several other applications, CDs possess qualities such as high solubility in aqueous media, strong luminescence, biocompatibility, functionalization, and chemical inertness. CDs are considered to be nanoparticles of semi-spherical shape with a crystalline graphitic center, prepared by thermal treatment ( $T > 300$  °C) of acceptable starting materials [6]. A number of methods for CDs production, including “top-down” and “bottom-up” experiments,

have been conducted. CDs were synthesized by the disintegration of carbonaceous materials such as carbon fibers, carbon nanotubes, and graphene in the top-down method. The bottom-up method, on the other hand, requires the polymerization of various aromatic compounds such as amino acids, citric acid, and carbohydrates. The techniques which have been used in the top-down approach include arc-discharge, ultrasonic synthesis, chemical ablation, laser ablation, and electrochemical oxidation, and bottom-up approach includes hydrothermal treatment, templated routes, thermal decomposition, microwave irradiation, plasma treatment, and electrochemical carbonization [5, 22]. The synthesis of carbon-based nanocomposites has been broadly researched to further increase the performance and efficiency of carbon quantum dots in the catalytic field [22]. Some of the dedicated reviews have been reported focusing on photocatalytic and electrocatalytic applications of CDs [5, 22, 23]. Recently, a dedicated review has been reported focusing green non-metal-doped CDs in nano-organocatalysis [4]. This review expounds focused study on the major research findings on zero-dimensional CDs (CQDs as well as CNDs)-based catalyst in several organic reactions, namely coupling reactions, oxidation, reduction, hydrogenation, heterocycle synthesis, multi-component reaction, cycloaddition, ring-opening, simple organic conversions.

## Types of carbon dots

Since CDs cannot be limited only to carbon NPs, it is necessary to classify the CDs, based upon their nanostructures. CDs can be broadly separated into carbon quantum dots (CQDs), carbon nanodots (CNDs), and graphene quantum dots (GQDs) [24]. Firstly, GQDs are 2D disc-shaped nanoparticles having one or few layers of graphene sheet obtained when there is the exfoliation reaction of graphitic materials. CQDs are quasi-spherical, multilayered nanoparticles with a graphitic crystalline core. The term “*quantum*” specifies nanoparticles with delocalized band structures, conceivably with the contribution of molecular-like and surface states. Nevertheless, CNDs are quasi-spherical, amorphous nanoparticles that have excited states derived exclusively from molecular-like species but do not demonstrate a quantum confinement effect. On the

other hand, distinguishing CQDs from CNDs might be quite difficult because it can be challenging to resolve the relative contributions from the excitation states and the structure. To accomplish this, it has been recommended that the word carbon dots (CDs) be used to represent any quasi-spherical carbon NPs, including those with delocalized electronic structure and molecular-like activity and also any carbon NPs ranging from CNDs and CQDs [25, 26].

## Characterization and properties

Characterization of carbon dots is critical for gaining a deeper knowledge of the mechanisms underlying these nanoparticles' distinctive physical features. However, due to the intricate nature of the reaction pathways, the precise chemical structures of CDs remain uncertain [1]. However, certain fundamental data can be acquired on a routine basis from specific techniques. Multiple approaches are utilized to characterize carbon dots and their physical properties, disclosing the crystalline arrangement of the carbon atoms, and testing the type and number of functional groups on the surface of CDs.

Transmission electron microscopy (TEM) has been a key tool for visualizing CDs which provides significant information on the shape of the particles, size distribution, and crystalline arrangement [27]. Furthermore, the crystallinity of graphitic CDs can be distinguished from amorphous CDs utilizing TEM or Raman spectroscopy [28]. The  $I_D/I_G$  intensity ratio of the typical Raman spectra can be utilized to investigate the assembly of the carbon framework, specifically the degree of crystallinity and relative abundance of core vs surface carbon atoms. High-resolution TEM studies were used to demonstrate the graphitic core's periodicity, which reflects its crystalline nature. Another important structural tool for determining the crystalline structure of carbon dots is X-ray diffraction (XRD) which offers data on the unit cell size and crystal spacing inside the crystalline carbon cores [27]. CDs obtained from several synthesis processes displayed distinct absorption peaks and stronger photoluminescence. The electronic properties of the CDs can be studied by optical spectroscopy through their photoluminescence (PL) or UV–Vis absorption. CDs often display noticeable optical absorption in the UV range with a tail covering into the visible range ascribed to  $\pi-\pi^*$  (C=C

bond) or  $n-\pi^*$  transition (C=O bond), or others [29–31].

CDs displayed stronger photoluminescence which includes piezochromic and solid-state up-conversion PL, phosphorescence, and fluorescence. CDs, for the most part, emit powerful blue emissions that swiftly diminish toward the red region. The PL characteristics of CDs are highly correlated with the conjugated core, surface state, molecular configuration, etc. While the quantum size effect does not appear to operate in most circumstances, the corresponding emission due to PL is mostly driven by the surface and defect state. The surface chemistry and the fabrication of CDs govern the QY of the CDs. As of now, the prominently enhanced QY value for CDs is 90% in solution. The PL has indeed been proposed to arise via a variety of mechanisms, which includes carbon excitons, size effect, surface groups, emissive traps, aromatic structures, edge defects, and free zigzag sites. Nevertheless, the precise mechanism of PL for CDs is obscure [1, 31, 32]. CDs' PL emission can be inhibited in the existence of either electron donors or acceptors, implying that CDs can operate as both electron donors and acceptors at the same time, which provides new insights for catalyst design. It is vital to evaluate the type and quantity of catalytically active species on the surface of the CDs. The application of several well-utilized analytical methods is employed to explicate the functional groups on the surfaces of CDs. X-ray photoelectron spectroscopy (XPS) delivers data on individual atomic units found on the surface of CDs and used to find out amino groups [33, 34]. FTIR spectroscopy is often used in conjunction with XPS to illuminate specific functional units by monitoring typical vibration bands. Furthermore, thermogravimetric analysis (TGA) can estimate surface group density and pyrolytic response of CDs at high temperatures by comparing mass loss at a given temperature with functional standardization on the surface of CDs [35].

With all of this info, it is possible to compute the catalytic stacking limit of the CDs in discussion and, inevitably, forecast the catalytic stacking for the functional groups specified. In addition as anticipated, because of the abundance of hydrophilic group on CDs interface, it shows high dispersions in H<sub>2</sub>O (polar solvents).

## Applications of CDs in organic synthesis

### CDs in C–C bond formation reactions

#### Suzuki and Heck reactions

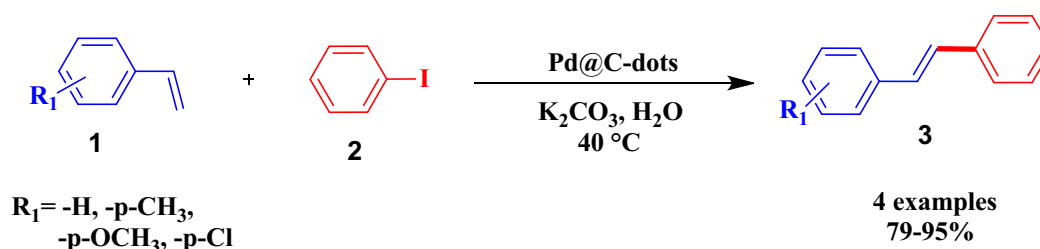
Carbon–carbon cross-coupling reactions catalyzed by Pd are regarded as one of the most effective and versatile methods in the field of synthetic organic chemistry. On the other hand, the variety of carbon forms on behalf of its huge surface area have been used as powerful support, for the dispersion of nanoparticles to protect nanoparticle agglomeration.

In continuation of this idea, Dey et al. in 2013 fabricated novel Pd@CDs composites in which the CDs were synthesized by thermal simmering treatment of clotted cream. The brown residue obtained was secluded from butter oil, dried, and then permitted to reflux (100 °C) through  $\text{H}_2\text{PdCl}_4$  in the presence of water yielding Pd@CDs. The CDs shells formed an ultrathin layer over Pd NPs. The hydroxy, epoxy and carboxyl groups on the CDs surface were responsible for the efficient reduction of  $[\text{PdCl}_4]^{2-}$  metal salt to form stabilized Pd NPs. The designed composite was used as a catalyst to investigate its efficiency in the reactions of Suzuki and Heck C–C coupling. But the catalytic performance was reduced due to incapability in the prevention of Pd agglomeration by CDs ultrathin layer. Hence, the authors reported the addition of a co-stabilizer such as PVP in small amounts to the Pd@CDs. The Suzuki reaction was performed with a Pd catalyst (0.5 mol%) in the presence of a base such as KOH in water at 60 °C offering biphenyls in 67–95% product yields. In addition, Heck reaction was carried out between styrene derivatives 1 and iodobenzene 2 by catalyzing with Pd (0.5 mol%) in the presence of  $\text{K}_2\text{CO}_3$  in water at 40 °C gave respective stilbenes 3 in 79–95% yields (Scheme 1). The as-synthesized composite was

recycled without significant agglomeration of Pd NPs for 3 cycles [36].

Owing to the high expense and toxic nature of Pd, there has been an increase in interest in the organization and usage of recoverable heterogeneous Pd catalysts in recent years [37–41]. To accomplish this, many solid materials were already been identified as heterogeneity support for Pd catalysts such as mesoporous materials [42], modified silicas [43], ionic liquids [44], polymers [45], and natural supports [46]. Despite major advances in this field, the separation and efficient recovery of the heterogeneous catalyst from the reaction medium using traditional methods such as filtration or centrifugation are not an easy task. The use of  $\text{Fe}_3\text{O}_4$  magnetic nanoparticles (NP) as a suitable support for heterogenization of Pd catalysts is one of the finest techniques to overcome that problem [47, 48]. The important features of magnetic-NP-supported catalysts are their ease of isolation and recovery, high surface area, and low toxicity. CDs bearing carboxylic and hydroxyl groups enable high water solubility and biocompatibility and provide excellent catalytic support and stabilization.

Therefore, in continuation with the work of Dey and group, Gholinejad et al. documented for the first time the synthesis of magnetic  $\text{Fe}_3\text{O}_4$  NPs-decorated CDs containing carboxylic acid and hydroxyl groups which were used for the Pd(II) reduction for the Pd NPs formation. The composite catalyst was prepared as follows: Hydrothermal treatment of citric acid and urea precursors in a Teflon autoclave at 160 °C was carried out to get CDs, and then, the obtained CDs were admitted to reacting with  $\text{Fe}_3\text{O}_4$  NPs in water at 60 °C to afford  $\text{Fe}_3\text{O}_4$ @CDs. Sonication followed by heating of  $\text{PdCl}_2$  and  $\text{Fe}_3\text{O}_4$ @CDs at 60 °C for 24 h in water provides Pd@ $\text{Fe}_3\text{O}_4$ @CDs. This powerful heterogeneous catalyst was employed in the Suzuki–Miyaura reaction between aryl boronic acids 4 and aryl halides 5 (Br, Cl) under the optimized condition of Pd (0.22 mol%) as the catalyst,  $\text{K}_2\text{CO}_3$  as the base,



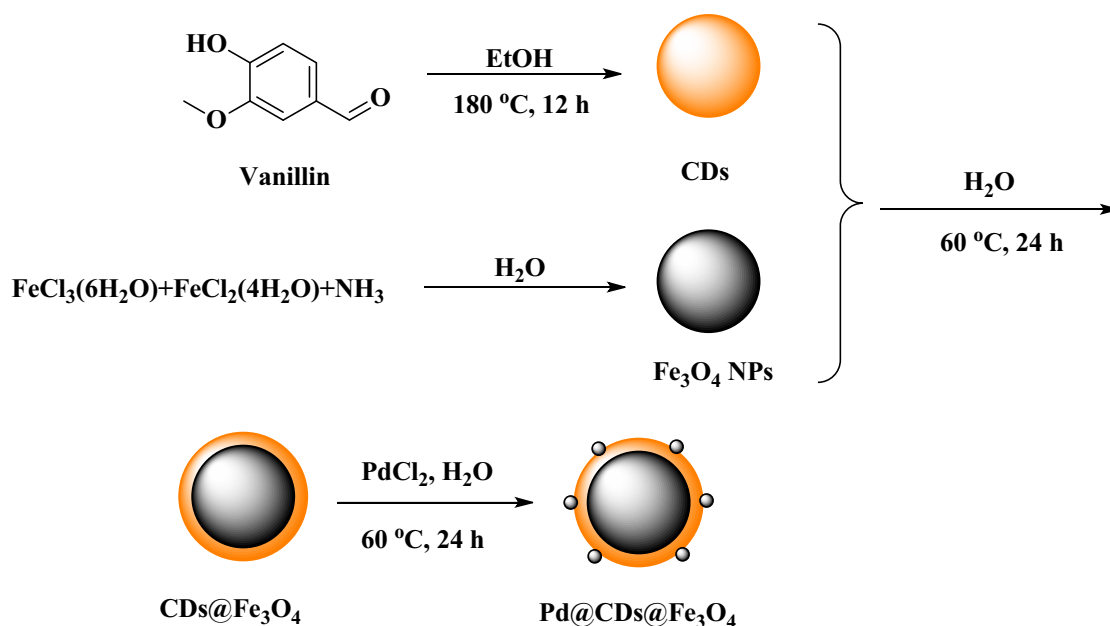
**Scheme 1** Pd@C-dot-PVP catalyzed Heck coupling.

and EtOH/H<sub>2</sub>O as the solvent to yield biphenyl derivatives **6** at r.t for aryl bromides and at 80 °C for aryl chlorides. Unsubstituted aryl bromides, heterocyclic aryl bromides, and aryl bromides bearing electronic substituents were well tolerated affording good yields. Even though aryl bromides gave better yields, aryl chlorides were more accessible to palladium-catalyzed cross-coupling reactions and also less expensive than aryl bromides. The CDs were thus clearly found to be more significant in the stimulation and stabilization of Pd NPs. It had also been shown that the catalysts assisted by magnetite-NPs provided easy separation and can be recycled without loss of catalytic activity for up to eight cyclic runs with little Pd leaching (1.26%) [49].

The same research group documented the synthesis of CDs from vanillin as it was a cheap and naturally abundant compound. Firstly, the CDs were synthesized by hydrothermal treatment of vanillin in EtOH at 180 °C in an autoclave at 12 h. Then, heating of CDs with Fe<sub>3</sub>O<sub>4</sub> NPs at 60 °C for 24 h followed by treatment of PdCl<sub>2</sub> in water at 60 °C for 24 h provides Pd@CDs@Fe<sub>3</sub>O<sub>4</sub> (Scheme 2). The catalytic performance of this nanohybrid (0.1 mol% Pd) was evaluated by testing it in the Suzuki reaction in accordance with the previously established reaction conditions. Reactions of aryl boronic acids with aryl bromides were performed under aq. EtOH at r.t, whereas PEG 200 was used as a solvent for aryl chlorides at 120 °C.

Aryl halides and aryl boronic acids bearing several electronic functional groups and heterocyclic aryl bromides were sustained well giving biaryl derivatives in good to excellent yields. Due to the superparamagnetic properties of Pd@Fe<sub>3</sub>O<sub>4</sub>@CDs nanohybrid, the catalyst was separated by an external magnet easily and recycled up to eight cycles with little decrease in its catalytic activity [50].

In 2016, Gholinejad et al. designed novel MgO-CDs as a fluorescent active catalyst to produce and stabilize palladium nanoparticles. To prepare MgO-CDs, Mg(NO<sub>3</sub>)<sub>2</sub> was dissolved in PEG 200 at r.t followed by the addition of aq. Na<sub>2</sub>CO<sub>3</sub> and urea mixture and then hydrothermal treatment of the mixture in an autoclave for 2 h at 160 °C. The resultant MgO-CDs were then heated with a mixture of aq. EtOH and PdCl<sub>2</sub> in water (sonicated) for 24 h at 60 °C affording Pd@MgO@CDs composite. Upon using 0.3 mol% of the designed catalyst, Suzuki reaction was performed between aryl boronic acids and aryl bromides under already described reaction conditions, giving biphenyls with excellent yields. Reactions with aryl chlorides afforded poor yields. Rising the reaction temperature to 80 °C, however, gave 72–98% product yields. Aryl bromides and boronic acids bearing various electronic functional groups were sustained well giving excellent yields. Due to the heterogeneous nature of the catalyst, the authors reported the recyclability of the catalyst up to 6 consecutive runs



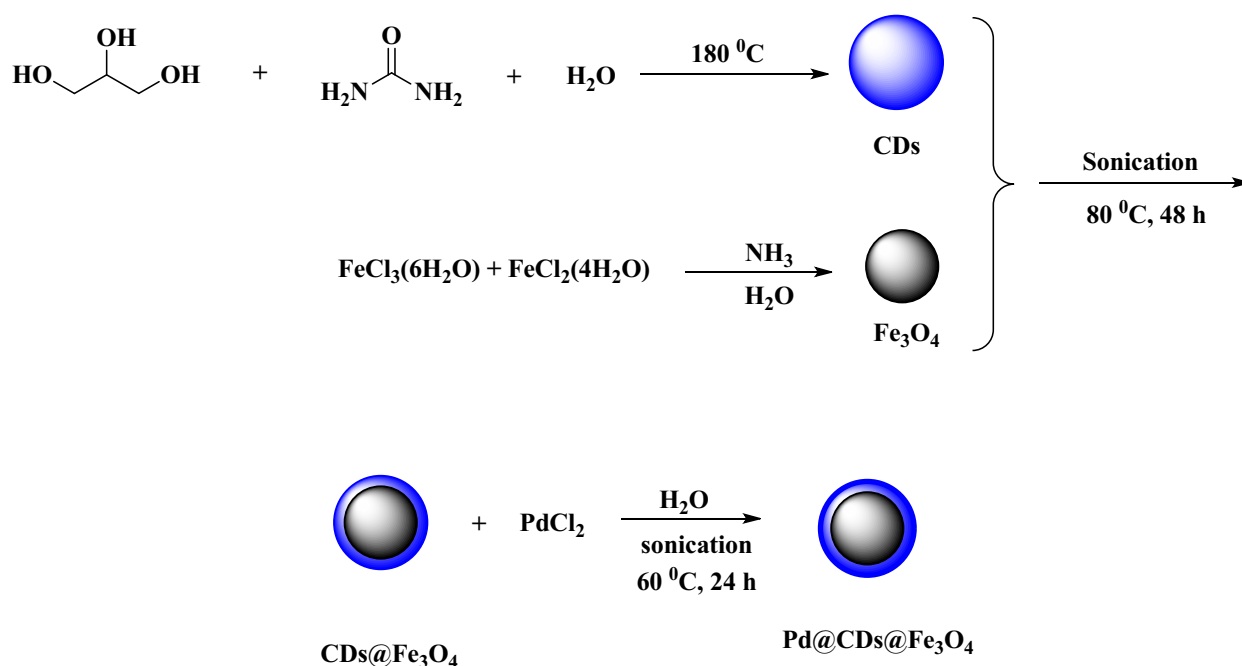
**Scheme 2** Synthesis of Pd@CDs@Fe<sub>3</sub>O<sub>4</sub> (CDs from vanillin).

with decreasing yields to 80% under optimized reaction conditions. Also, the author demonstrated a new protocol to detect the loading of palladium by measuring the MgO-CDs fluorescence emission and leaching during the catalyst production and recycling process. The results demonstrated that increasing the Pd loading on MgO-CDs lowered fluorescence emission due to electron transfer from the CDs to metallic ions. It is feasible to compute the Pd amount on the support in each stage by using a linear relationship between the content of supported Pd and emission [51].

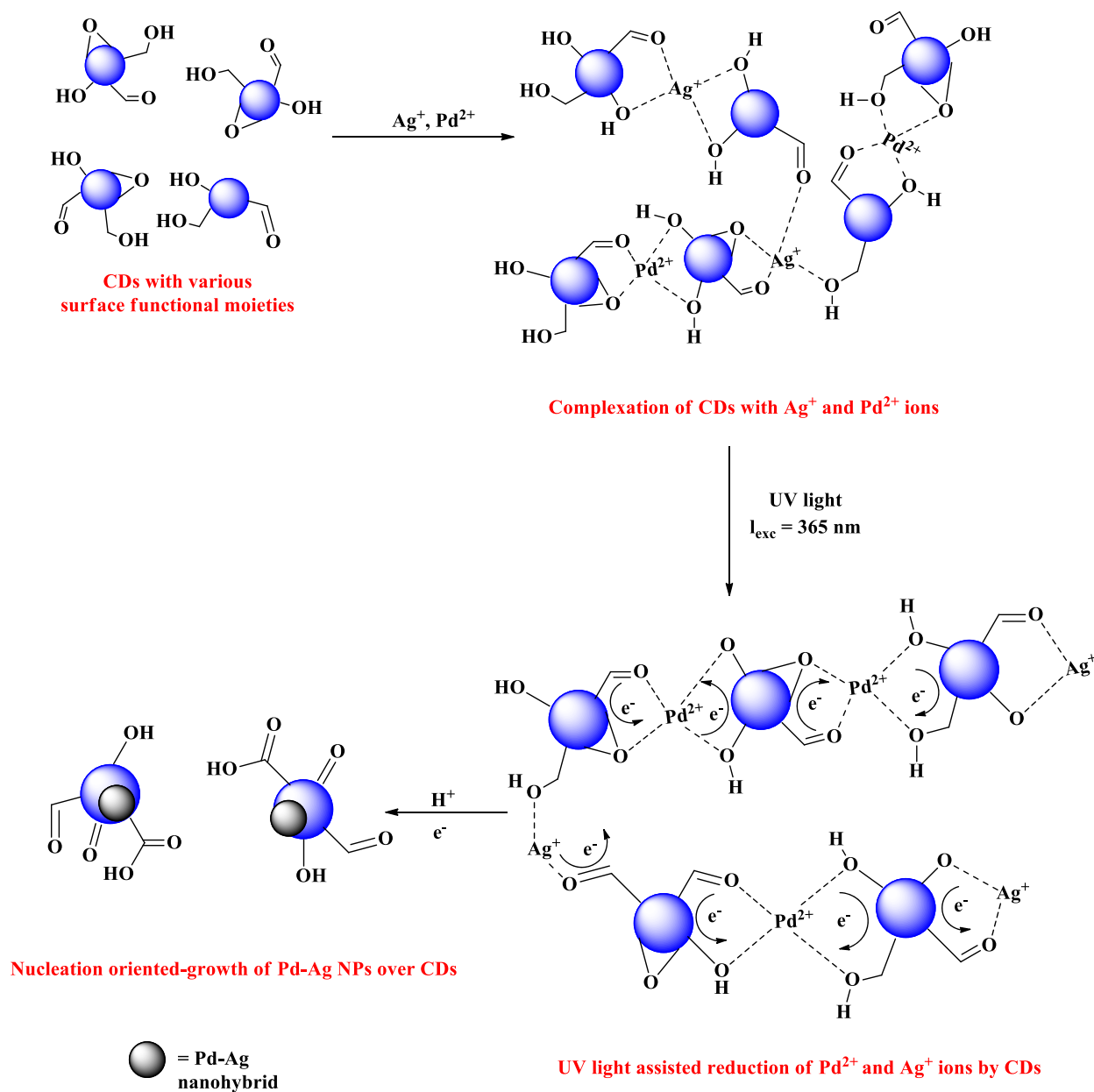
In 2017, Gholinejad et al. focused on Suzuki–Miyaura coupling reactions using the same catalyst Pd@CDs@Fe<sub>3</sub>O<sub>4</sub>. But the source of the CDs was different, as it was prepared from glycerol and urea in a green manner, and the composite was prepared as illustrated in (Scheme 3). Initially, the reaction between 4-bromoanisole and phenylboronic acid was chosen as a typical reaction to investigate the optimized reaction condition. Results showed that on using Pd catalyst (0.3 mol%), the equivalent mixture of water and ethanol as a solvent and t-BuOK as a base gave biphenyl with 92% yield. Aryl bromides bearing several functional electronic groups were well sustained giving excellent yields, and also, heterocyclic compounds such as 2-bromopyridine and 5-bromopyridine gave the coupling products in

82–90% yields. Similarly, several reactions were examined with potassium phenyltrifluoroborate (4 examples) instead of aryl boronic acid which gave a product yield of 94–83% yields, and substituted aryl diazonium tetrafluoroborates (5 examples) gave desired product in 91–88% yields. The authors reported that this magnetic catalyst can be easily separated for more cycles with no significant loss in catalytic activity particularly 10 cycles for the reaction between iodoanisole and phenylboronic acid with the Pd and Fe leaching of 16% and 0.2%, respectively. The exact essence of the catalyst in the Suzuki reaction was also determined utilizing various assays to be a homogenous system. [52].

Bayan et al. in 2017 developed UV–visible (365 nm) intervened synthesis of Ag–Pd bimetallic nano hybrid on CDs in which the CDs were obtained from microwave-assisted hydrothermal treatment of D-glucose. Herein, due to the presence of various surface functionalities such as hydroxyl, alkoxy, carboxylic, aldehydic, and carbonyl groups on its surface, CDs were employed to stabilize and reduce Ag<sup>+</sup> and Pd<sup>2+</sup> ions (Scheme 4). The physicochemical characteristics of the nano hybrid have been assessed by FTIR, EDX, UV–Vis, XRD, and TEM analyses. The catalytic efficiency of the nano hybrid was tested in Suzuki reaction under ambient and ligand-free conditions. The best reaction condition was 5 wt% of the



**Scheme 3** Synthesis of Pd@CDs@Fe<sub>3</sub>O<sub>4</sub> (CDs from glycerol and urea).



**Scheme 4** Synthesis of Pd-Ag@CDs nano hybrid.

catalyst,  $\text{K}_2\text{CO}_3$  as a base, and ethanol-water as a solvent in the coupling reaction of 4-bromoanisole and 4-ethylphenylboronic acid affording 4-ethyl-4'-methoxy-1,1'-biphenyl with a 94% isolated yield. With that optimization condition in hand, the reaction between structurally distinct aryl boronic acid and aryl halide has been carried out to produce the corresponding biaryl product. However, the results showed that the rate of the reaction relies on the nature of the substituents bearing in both the reactants. It had been attributed that aryl boronic acid and also aryl halides with electron-releasing groups

facilitated the reaction and required lesser completion of time for the reaction to occur, whereas the presence of electron-withdrawing substituents required a longer completion time. Also, it was seen that the reaction with aryl bromides gave a high yield of 97%, while aryl chloride gave a poor yield of 25%. This could be ascribed to the existence of electron-releasing polar groups on the surface of the CDs in the nano hybrid, which can better interact with the compounds having electron-donating groups promoted the reaction to better yields than those having electron-withdrawing groups. Moreover, bimetallic



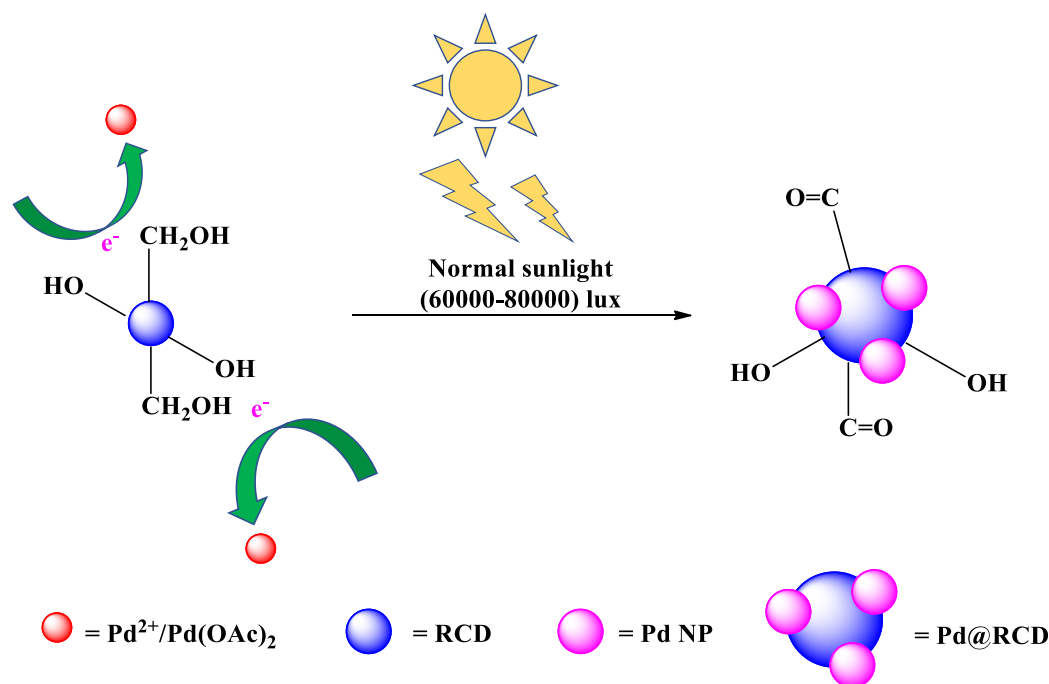
Ag-Pd@CDs nanohybrid showed excellent catalytic activity in comparison with the individual assistance of PdNPs, AgNPs, and CDs. Also, it had been noted that this heterogeneous nanohybrid catalyst can be separated and recycled for up to six cycles [53].

Duarah et al. in 2019 designed palladium-reduced CDs (10–15 nm) incorporated in starch-based HPU nanocomposites, which were fabricated by in situ polymerization approach as described in the scheme. The nanohybrid was synthesized using a one-pot strategy that merged Pd nanoparticles with reduced CDs without any need for toxic substances or rigorous conditions (Scheme 5). The reduced CDs in the as-prepared catalyst with the HPU matrix elevated the tensile strength (twofold), thermal stability (by 25 °C), and toughness (3.5-fold) of the hyperbranched polyurethane than the pure one. The designed composite existed as a visible light photocatalyst which was employed in the Suzuki–Miyaura reaction to synthesize biphenyl derivatives. It had been observed that better yields of 80–97% were reported for the reactions between aryl boronic acids and aryl iodides containing both electron-withdrawing and electron-donating groups. The designed catalyst was reported to be recycled and can be reused; however, a

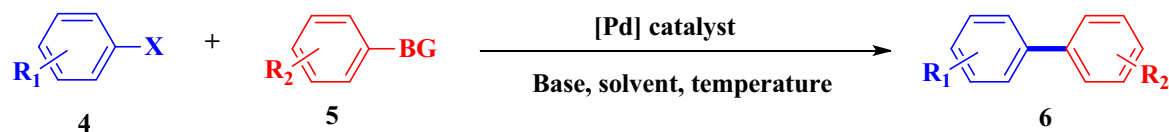
minimum loss of the catalyst was observed due to the degradation of the catalyst [54]. The typical Suzuki–Miyaura reaction was shown in (Scheme 6).

#### *Knoevenagel condensation*

The carbon–carbon bond formation between the active methylene group and aldehydes or ketones is called the Knoevenagel reaction. Knoevenagel products are often used to make coumarin derivatives, cosmetics, fragrances, medicinal substances, and polymers, and so on [55–57]. As of now, several Lewis acids and bases have traditionally been utilized as homogeneous catalysts [58–62]. Though homogeneous catalysts have separation and recyclability issues, many attempts have been devoted in utilizing heterogeneous systems like molecular sieves [63] organic functionalized molecular sieves, or silica [64–66] metal–organic frameworks (MOF) such as UiO-66 [67], Zif-8 [68], Zif-9 [69], IRMOF [70], and mixed oxides nanoparticles [71] which were indeed active for Knoevenagel condensations. Because of the basic nature of CD surfaces, attempts have been made to employ this form of CDs as a catalyst for Knoevenagel reactions.



**Scheme 5** Synthesis of Pd@RCD.



$\text{X} = \text{Br, Cl, I, N}_2^+\text{BF}_4^-$

$\text{G} = (\text{OH})_2, \text{F}_3\text{K}$

$\text{R}_1 = \text{aryl, heteroaryl, alkyl, EWG, EDG, etc.}$

$\text{R}_2 = \text{EWG, EDG, etc.}$

**Scheme 6** Typical Suzuki–Miyaura reaction.

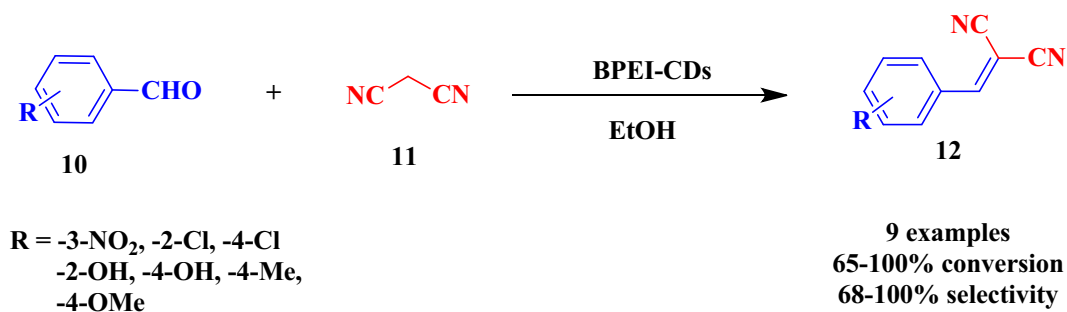
Xiaoyan Pei et al. in 2018 synthesized different types of amine-terminated CDs by pyrolyzing a mixture of citric acid and appropriate diamines at 180 °C in 1-octanol for 6 h under argon and then purifying them with water, to check its reverse-phase transfer nature between the aqueous phase and organic phase using CO<sub>2</sub> bubbling. The catalytic efficiency of the synthesized 1,4-diaminobutane (DAB)-CDs was tested by using it as a catalyst in Knoevenagel reaction between 4-bromobenzaldehyde 7 and malononitrile 8 to give the desired coupling product 2-(4-bromobenzylidene) malononitrile 9 in 1-octanol organic phase system at 45 °C (Scheme 7). The authors concluded that the CDs bearing primary amines facilitate condensation processes more effectively than those with secondary or tertiary amines with respective yields of 95.2, 81.1, and 75.3%. After accomplishment of the reaction, the suspended outcome in the organic phase can be filtered upon adding CO<sub>2</sub> bubbles so that the CDs were transferred to the aqueous phase. Again, CO<sub>2</sub> could be removed upon N<sub>2</sub> bubbling. According to <sup>13</sup>C NMR spectra, the authors proposed that the driving factor for such a reversible phase transfer was the reversible acid–base reaction of CDs bearing amines with CO<sub>2</sub> and the reversible production of hydrophilic ammonium ions. The same reaction can be carried out again with the same reaction phase. The amine-terminated CDs gave a 93.7% yield for 6

consecutive cycles. The reported catalyst ensured homogeneous reaction and heterogeneous separation [72].

Farzaneh et al. in 2020 prepared branched polyethyleneimine capped CDs (BPEI-CDs), as a solid catalyst, by carbonization of CA with BPEI precursor at 200 °C, with size ranging from 5 to 10 nm. The reported catalyst was employed to be an excellent heterogeneous catalyst for the Knoevenagel condensation of diverse benzaldehydes 10 with malononitrile 11. Also, it drives this condensation due to the basic nature of the surface of CDs. Several experiments have been made in finding the optimization reaction condition. Thus, it was observed that on using 25 mg catalyst loading, ethanol as solvent at 60 °C for 2 h increased the benzaldehyde conversion to benzylidene malononitrile 12 (Scheme 8) with 100% conversion and selectivity. These results indicated that an increase in reaction temperature and high polar solvent enhanced this condensation. With this optimized condition, the condensation of benzaldehyde substrates with malononitriles has been made. Noticeably, benzaldehyde and substituted benzaldehyde with electron-withdrawing groups at meta and para position enhanced the conversion and selectivity to the product, whereas electron-releasing groups retarded the conversion and selectivity resulted in poor yields. This poor conversion and selectivity could be attributed to the destabilization of



**Scheme 7** DAB-CDs catalyzed Knoevenagel condensation.



**Scheme 8** BPEI-CDs catalyzed Knoevenagel condensation.

the intermediate. But, in case of 2-hydroxy benzaldehyde containing an electron-donating hydroxyl group offered better conversion and selectivity. It is due to the hydrogen bond formation between carboxylate and hydroxyl group. Due to the heterogeneity of the catalyst, it can be retrieved, recycled, and reused. Also, the catalyst retained its catalytic activity with no significant loss for 3 consecutive runs [73].

#### Sonogashira reaction

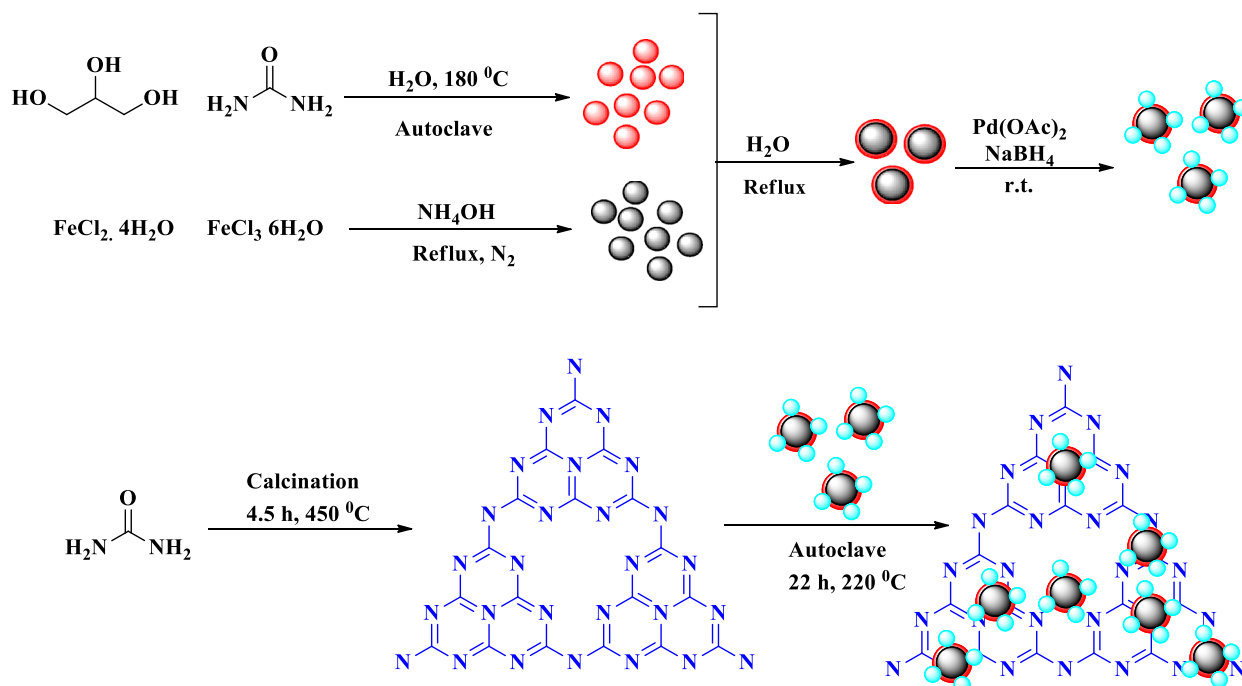
One of the most interesting ways for manufacturing significant components such as various polymers, natural products, and pharmaceutical compounds is the coupling reaction, particularly the Sonogashira coupling reaction [74]. Traditionally, the Sonogashira coupling reaction is carried out in the presence of a co-catalyst, such as copper, phosphine ligands, and palladium catalyst, with THF/toluene as the solvent in an inert atmosphere [75]. The use of homogeneous Pd catalyst has various drawbacks, the most notable of which are the time-consuming recovery and recyclability of the catalyst, product contamination, and the loss of expensive Pd catalysts. As a result, the disclosure of cost-effective and environmentally acceptable heterogeneous catalytic systems, as well as the development of copper and ligand-free techniques, has piqued attention [76, 77]. For the catalytic properties of Pd NPs, the particle size and active atoms on the catalyst surface are the two main parameters [78, 79]. Carbonaceous materials have opened up new avenues for novel applications in heterogeneous catalysis, resulting in improved conversions and reaction selectivity.

Therefore, Mohammadi et al. in 2019 accomplished hybridization of g-C<sub>3</sub>N<sub>4</sub> (promising heterogeneous catalyst support) with CDs to enhance the catalytic

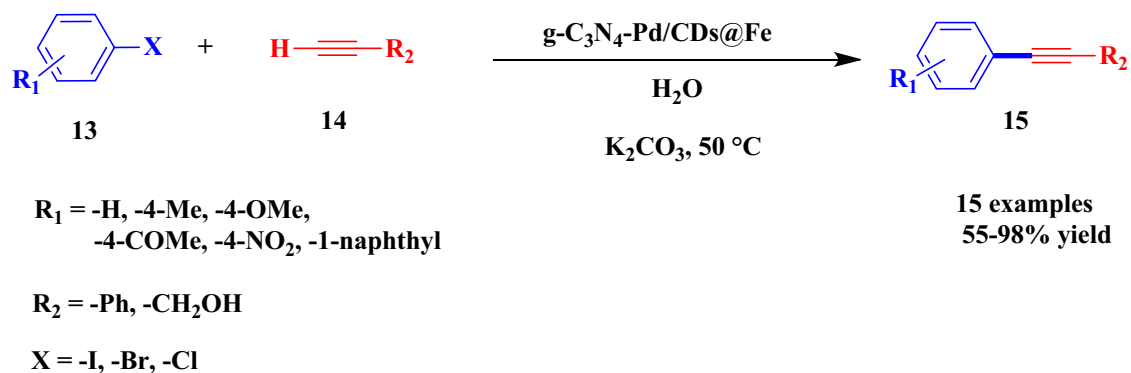
activity through synergism and stabilization of Pd NPs in the g-C<sub>3</sub>N<sub>4</sub>-Pd/CDs@Fe novel hybrid efficient catalyst (Scheme 9). Hence, they carried out the Sonogashira cross-coupling reaction as a co-catalyst free reaction utilizing the reported catalyst. The authors have chosen the reaction of iodobenzene 13 and phenylacetylene 14 to yield the corresponding coupling product 15 as a typical Sonogashira coupling to find the optimized reaction condition, and 20 mg of g-C<sub>3</sub>N<sub>4</sub>-Pd/CDs@Fe was used as a catalyst, K<sub>2</sub>CO<sub>3</sub> as a base, water as solvent at 50 °C promoted the reaction with an excellent yield of 95%. It was reported that the inclusion of g-C<sub>3</sub>N<sub>4</sub> to Pd/CDs@Fe significantly enhanced the coupling reaction due to the synergism of the components in the hybrid. They conducted some experiments with structurally different aromatic and aliphatic acetylene and halo benzenes. It was observed that electron-withdrawing groups such as the acetyl group in aryl iodide enhance the reaction toward a better yield of 98%, and also, aromatic acetylene was superior to the aliphatic acetylenes (Scheme 10). Also, the reaction of aryl chloride with aromatic acetylene gave the coupling product, and a poor yield of 55% was obtained. The catalytic activity of g-C<sub>3</sub>N<sub>4</sub>-Pd/CDs@Fe was retained for 3 consecutive runs, and deterioration in the catalytic activity was observed after 4 runs. As the catalyst comprises iron, it can be magnetically separable and reused [80].

#### Cross-coupling reaction

Sarma et al. in 2019 reported sulfur-doped CDs (s-CDs) as a catalyst in the photoinduced cross-dehydrogenative coupling reaction of benzyl hydrocarbons 16 and nucleophiles 17 such as ketones and arenes to give the desired coupling product 18 (Scheme 11) in maximum yield of 96% within 12 h

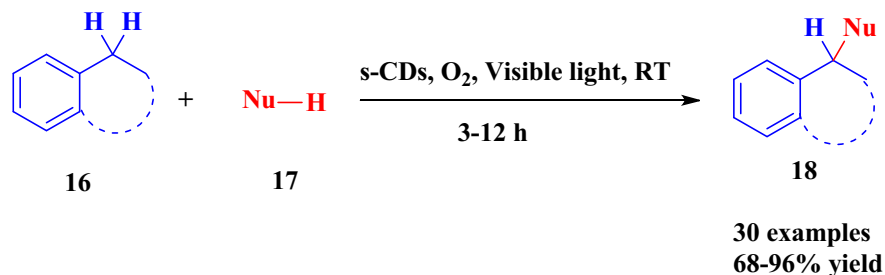


**Scheme 9** Synthesis of  $g\text{-C}_3\text{N}_4\text{-Pd/CDs@Fe}$  nano hybrid.



**Scheme 10** Sonogashira coupling of various halides using  $g\text{-C}_3\text{N}_4\text{-Pd/CDs@Fe}$ .

**Scheme 11** s-CDs catalyzed aerobic C–C coupling reaction.



of reaction time upon 425 nm, 34 W blue light irradiation in a solvent-free and oxygen environment. The reactions were performed in the absence of the oxygen or catalyst and dark provided a

lesser product yield of below 31% ensuring the role of photocatalytic activity of s-CDs. Finally, the catalyst can be recycled for 4 runs with no significant loss in its catalytic activity [81].

## CDs for ipso-hydroxylation

Bayan and Karak in 2018 developed a bio-based nanocomposite by supporting Pd–Ag@CDs in hyperbranched polyurethane matrix (HPUNCs) to investigate its catalytic ability in the *ipso*-hydroxylation by oxidation of aryl boronic acid. The best-optimized reaction condition was reported using 5 wt% of HPUNC catalyst loading and 0.15 ml of 30% H<sub>2</sub>O<sub>2</sub> oxidant which conferred 100% conversion efficiency in the conversion of phenylboronic acid **19** to phenol **20** (Scheme 12) within 30 min of reaction time at r.t in the presence of a solvent such as water. Further, the scope of the designed catalyst was extended by investigating the reaction of various aryl boronic acid substrates afforded a maximum yield of 90–100%. Furthermore, the catalytic efficiencies of pristine HPU, Pd–Ag/CDs nanohybrid, and HPUNCs were compared. Out of those, HPUNCs exhibited better conversion efficiency with ease of recovery of the catalyst. The main role of CDs in this catalyst was: It provided dispersion of metal nanoparticles in the polymer matrix by the interaction of its surface functional groups [82].

## CDs for oxidation reactions

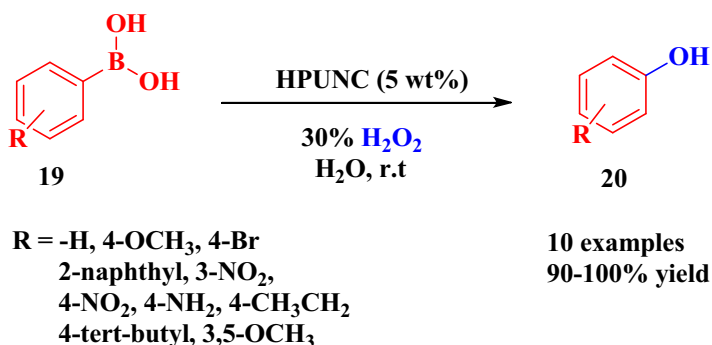
Organic chemistry is paying a lot of attention to the green oxidation of organic molecules to their high-value-added products under mild conditions. The selective conversion of alcohols to their respective carbonyl compounds is particularly important in organic synthesis, as the resulting molecules are incredibly useful intermediates in the pharmaceutical and fragrance industries [83–85]. However, in conventional industrial production, stoichiometric oxidants include permanganate and perchlorate and were widely utilized in homogeneous reactions.

Noble metal and metal oxide-based catalysts including Ru [86], Ag [87], Au [88, 89], Pd [90, 91], RuO<sub>2</sub> [92], and MnO<sub>2</sub> [93] were also developed to achieve high selectivity and activity. However, noble metal or metal oxides have drawbacks such as relatively expensive costs and environmental pollutions.

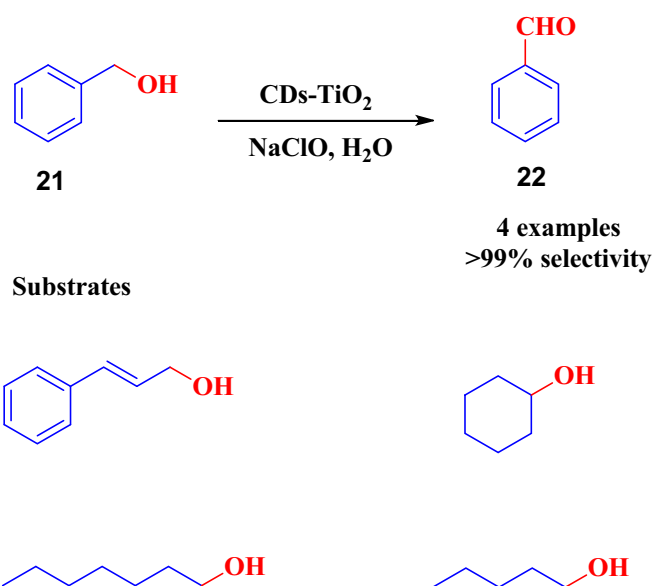
Thus, in the year 2016, Zhang et al. carried out the oxidation of benzyl alcohol and other distinct alcohols in water using CDs that were free from transition metal. Herein, CDs were prepared from graphite rods by a one-pot facile electrochemical method. In addition, the authors compared the catalytic efficiencies of CDs, graphene, and carbon nanotubes under the optimized condition of 0.5 g of the catalyst and 10 ml of an oxidant such as NaOCl at 70 °C in the oxidation of benzyl alcohol, cyclohexanol, cinnamic alcohol, and N-octanol. Out of those, N-octanol was converted with 100% efficiency to n-caprylic aldehyde within 6.5 h. CDs showed the best conversion due to their fine particle size and a huge amount of surface oxygen-carrying groups, made them superior to other above-mentioned catalysts. Moreover, the CDs can be recycled and reused for another set of oxidations [94].

Though CDs displayed excellent catalytic activities in the oxidation of alcohols, the nanosize of CDs causes aggregation during the reaction. Hence, the same research group in 2017 used TiO<sub>2</sub> as solid support for the effective dispersion of CDs to carry out the oxidation of aromatic and aliphatic alcohols **21** to yield the corresponding oxidized product **22** (Scheme 13). The same reaction condition was maintained with the use of CDs–TiO<sub>2</sub> nanocomposite as a catalyst. The composite was prepared by the simple hydrothermal method. It had been observed that 67 wt% of the CDs–TiO<sub>2</sub> catalyst was the optimal reaction condition. Oxidations of distinct alcohols have been reported. Furthermore, it had been noted

**Scheme 12** *ipso*-hydroxylation of aryl boronic acids.



**Scheme 13** Oxidation of alcohols using CDs-TiO<sub>2</sub> Nanocomposites.



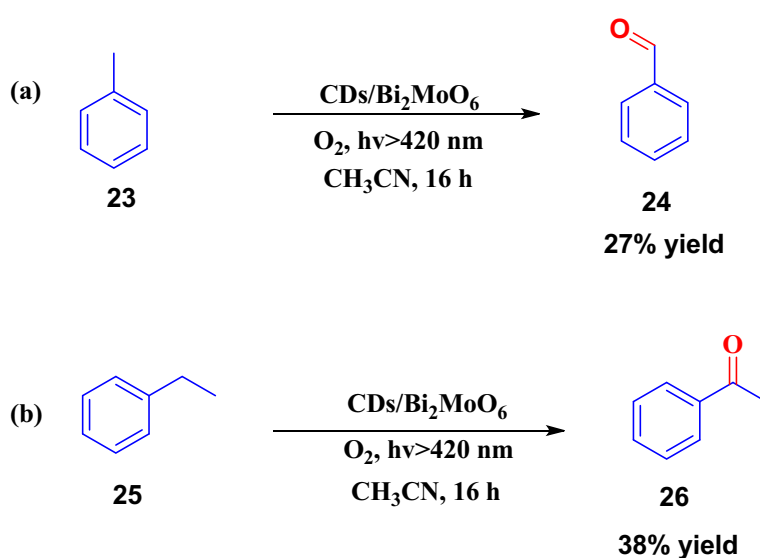
that 100% conversion and greater than 99% selectivity were found for the oxidations of n-amyl alcohol and n-octanol and also other reported alcohols. Owing to the heterogeneous nature of the designed catalyst, the separation was easy and can be run for 5 consecutive cycles with no loss of catalytic activity [95].

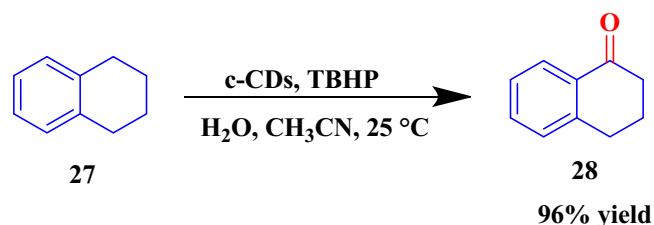
Subhajyoti Samanta and team in 2017 prepared CD/Bi<sub>2</sub>MoO<sub>6</sub> nanocomposite by embedding carbon dots onto the nanoplates of Bi<sub>2</sub>MoO<sub>6</sub> and examined its photocatalytic activity in the oxidation of toluene 23 to benzaldehyde 24 (Scheme 14a) and the oxidation of ethylbenzene 25 to acetophenone 26 (Scheme 14b). Under the optimal conditions of 2.4 wt% of the catalyst, 10 W LED as light source,

acetonitrile as a solvent in the presence of oxygen, the reaction produced products with yields of 27% and 38%, respectively [96].

In the year 2018, Sarma et al. investigated the conversion of alkyl benzene by photooxidation using CDs functionalized with carboxyl groups (c-CDs) as a catalyst. The use of TBHP as an oxidizer, a mixture of CH<sub>3</sub>CN and H<sub>2</sub>O as a solvent, and a 60 W LED as a light source was reported to provide 96% yield with 99% selectivity in oxidation in the conversion of tetralin 27 to tetralone 28 (Scheme 15). With the optimal condition, photooxidation of different benzylic hydrocarbons, xanthene derivatives, and N-heterocyclic compounds had been performed which

**Scheme 14** Photooxidation to benzaldehyde (a) and acetophenone (b).

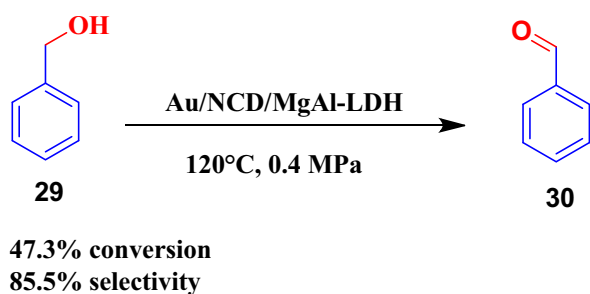
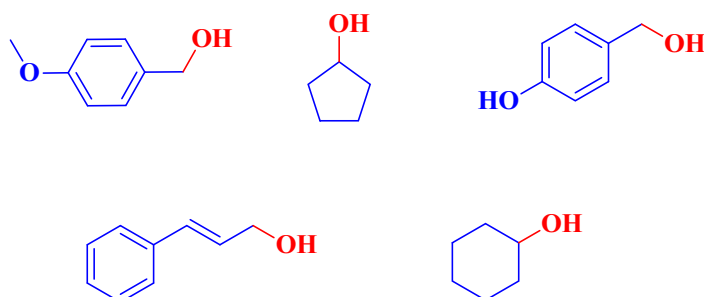


**Scheme 15** Photooxidation of benzylic hydrocarbons.

resulted in better conversion and selectivity. But, in the case of oxidation of heterocyclic moiety with pyridinic structure, a lower yield was observed. Also, comparative performance of r-CDs and n-CDs with c-CDs was made and the output of the results indicated c-CDs were significant in C–H photooxidation by promoting efficient electron transfer to substrates by suppressing electron–hole pair recombination [97].

In 2020, Guo et al. reported for the first time on the oxidation of benzyl alcohol 29 to benzaldehyde 30 in solvent- and base-free conditions utilizing nitrogen-doped CDs incorporated in 2D-layered Mg–Al double hydroxide supported with Au nanoparticles (NCD/Au/MgAl-LDH) as nanocatalyst. (Scheme 16). Comparative performance of NCD/Au/MgAl-LDH and pristine Au/MgAl-LDH on the benzyl alcohol conversion without using solvent and base had been made. The results showed that the enhancement in the conversion (47.3%) and selectivity (85.5%) to the

product benzaldehyde with the TOF ( $20,175 \text{ h}^{-1}$ ) was observed for NCD/Au/MgAl-LDH with Au loading of 0.82% over pristine Au/MgAl-LDH which results in only 38.2% conversion and 84.5% selectivity to the product. This excellent catalytic activity of the reported catalyst was attributed to the powerful interaction between Au NPs and NCD/MgAl-LDH nanohybrid because the NCD introduction facilitated dispersion on the 2D LDH uplifted the surface basicity leads to the activation and adsorption of benzyl alcohol toward oxidation. Furthermore, oxidation of benzyl alcohol with NCD/Au/MgAl-LDH had been carried out in the presence of toluene as solvent. Even though better conversion ( $> 99.0\%$ ) and selectivity ( $> 94.0\%$ ) to product benzaldehyde had been observed, however, lower TOF value indicated the superiority of this catalyst in a solvent-free environment. Several experiments have been made to extend the scope of the reported catalyst using toluene as solvent under an oxygen pressure of

**Scheme 16** Oxidation of benzyl alcohol using Au/NCD/MgAl-LDH catalyst.**Substrates**

0.4 MPa over the oxidation of diverse alcohols. It had been observed that better conversion (80.4–99%) and selectivity (94.6–99%) to the corresponding oxidized product revealed the flexible nature of the NCD/Au/MgAl-LDH nanocatalyst [98].

Prathibha et al. in 2020 investigated controlled oxidation of benzylic alcohol using manganese dioxide as an oxidant as it can be recycled when it was stabilized with solid magnetic support and could do controlled and selective oxidation. To prevent loss of magnetism and agglomeration of  $\text{Fe}_3\text{O}_4$  nanoparticles, the authors reported the coating of these nanoparticles with CDs, as a stabilizing agent owing to its rich surface functional groups. To find the optimization condition, oxidation of *p*-methoxy benzyl alcohol had been carried out and it was reported that the use of 20 mol% of  $\text{Fe}_3\text{O}_4/\text{CDs}/\text{MnO}_2$  as a catalyst, molecular oxygen  $\text{O}_2$  as an oxidant, and toluene as solvent at 100 °C offered the corresponding aldehyde product with 100% selectivity in oxidation. Hence, the prepared  $\text{Fe}/\text{CDs}/\text{MnO}_2$  nanocomposite was incorporated in the oxidation of diverse aromatic alcohols 31 to corresponding aldehydes 32 under optimized reaction conditions. It had been noted that benzyl alcohols with both electron-withdrawing and electron-releasing substituents gave good to better yields. Halo-substituted benzyl alcohol gave a moderate yield of 58–64%, while 3-pyridinemethanol offers 62% yield (Scheme 17). Also, it had been observed that secondary benzyl alcohols oxidized to the corresponding ketone with a moderate yield of 75%. But, oxidation of allyl alcohol resulted in no reaction and also 4-(methylthio) benzyl alcohol oxidation resulted in 4-(methylthio) benzaldehyde as the oxidized product instead of resulting in 4-(methylsulfinyl) benzaldehyde or 4-(methylsulfinyl) benzyl alcohol as the oxidation product. This indicated the selectivity of the catalyst toward the oxidation of benzylic alcohols. It is possible to isolate the catalyst using an external magnet, and the recyclability of the catalyst was evaluated under optimized reaction conditions with the oxidation of *p*-methoxy benzyl alcohol. Thus, it had been observed from this test that the catalytic activity remained the same with no such significant loss for 5 cycles [99].

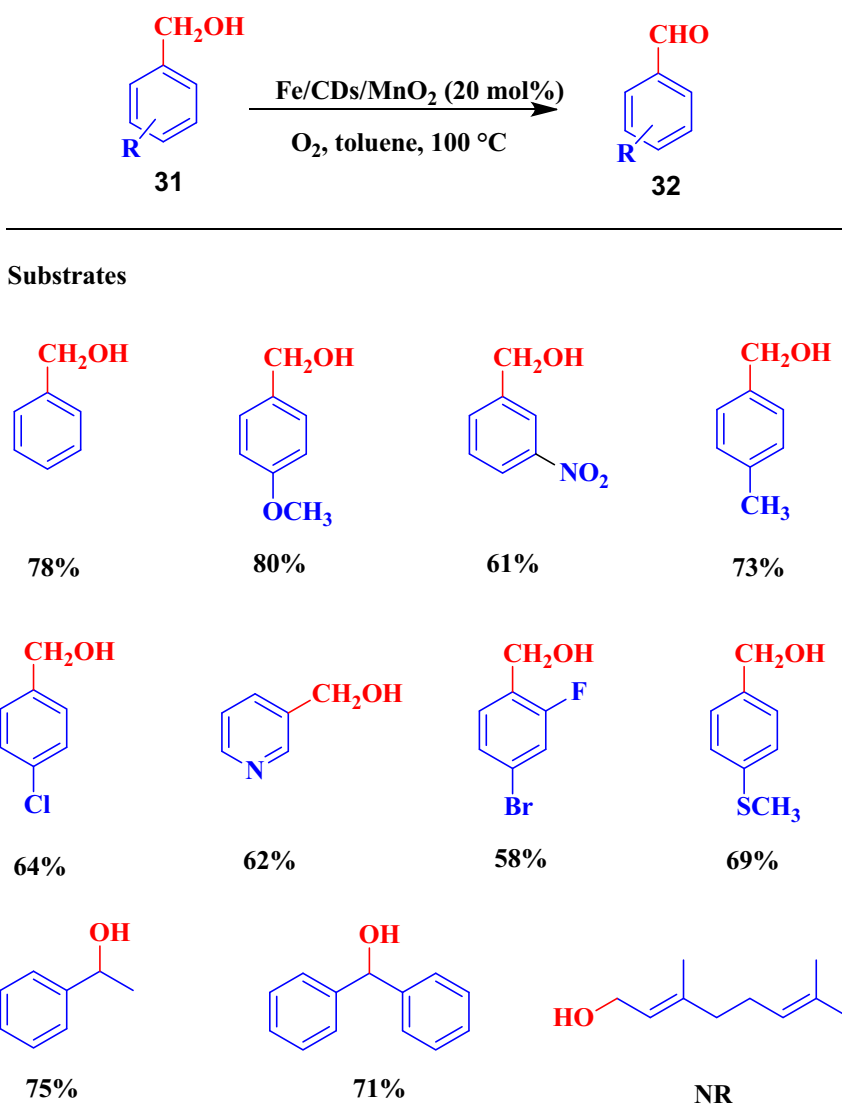
Mohammadi et al. in 2019 designed a heterogeneous novel nanocatalyst ( $\text{CDs}@IL/\text{WO}_4^{2-}$ ) by immobilizing tungstate ions ( $\text{WO}_4^{2-}$ ) in the CDs surface modified with [APMim][Cl]. The prepared

catalyst, in this literature, was reported as a powerful green heterogeneous catalyst for selective oxidation of alcohols 33 with high selectivity, to aldehydes and ketones 34 in the presence of  $\text{H}_2\text{O}_2$  as an oxidant without further oxidation to the carboxylic acid. In this report, benzyl alcohol oxidation was taken as a typical reaction in finding optimized reaction condition and it was observed that on using 10 mg loading of  $\text{CDs}@IL/\text{WO}_4^{2-}$  catalyst,  $\text{H}_2\text{O}/\text{CH}_3\text{CN}$  (1:1) as the solvent and 4 mmol of  $\text{H}_2\text{O}_2$  as oxidant under a temperature of 70 °C for 2 h gave highest conversion efficiency and yield of 95%. With this optimized reaction condition, oxidation of diverse alcohols has been reported (Scheme 18). Hence, it had been observed that 100% selectivity in oxidation with no acidic products and also relative product yields were observed. The reusable nature of the designed catalyst was evaluated by testing in benzyl alcohol oxidation under optimized conditions. The results showed that the designed catalyst can be reused for 5 successive cycles with minimum loss in its catalytic activity. In this report, the novelty of this catalyst was the ionic liquid modified CDs which could be regarded as excellent support for the stabilization of catalytically active species for the design of a new catalytic system, and also, it prevented nanoparticle agglomeration which lowered the catalytic activity [100].

In continuation of the past work described, water is being developed as a green solvent to replace organic solvents in organic transformations; nonetheless, water's limited ability to dissolve organic compounds is the fundamental problem. To overcome this issue, in this report, the same group successfully developed  $\text{CDs}@DDA\text{-IL}/\text{Cl}$  by hydrothermal one-pot synthesis of multi-functional CDs as amphiphilic catalyst constituted [APMim][Cl] (ionic liquid), DDA, and CA, which then anchored with tungstate ions using an anion-exchange method to produce  $\text{CDs}@DDA\text{-IL}/\text{W}$ , which was used for the effective oxidation of alcoholic substrates. The main advantages of this catalyst are to provide hydrophobic/hydrophilic balance in the aqueous medium without using any phase transfer catalyst, organic solvents, or any other additives with 100% selectivity in oxidation, greater TON(719), and TOF(479) with high yield. Furthermore, faster oxidation of alcohol 35 to the corresponding aldehyde and ketone 36 with no further oxidation was also observed (Scheme 19). The scope



**Scheme 17** Oxidation of diverse benzyl alcohols using Fe/CDs/MnO<sub>2</sub> nanocomposite.

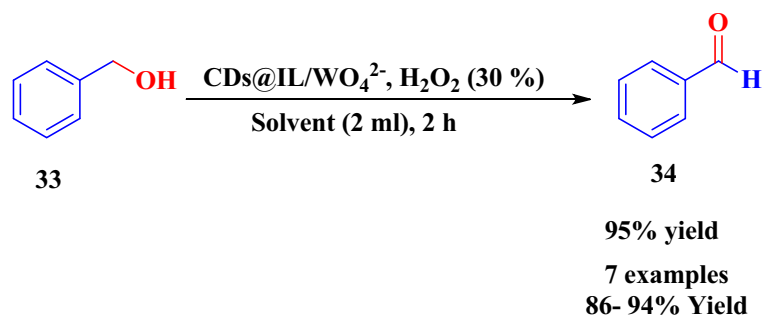


of the designed catalyst was used to investigate selective oxidation of different alcoholic substrates under optimized reaction conditions with the use of 8 mg loading of CDs@DDA-IL/W, 30% H<sub>2</sub>O<sub>2</sub> (3 mmol), water (2 mL) as solvent under a temperature of 70 °C. The results indicated that out of those all-alcoholic substrates, benzyl alcohol favored oxidation with excellent return of 97% though 2-butanol gave a minimum yield of 89%. Moreover, this catalyst facilitated oxidation of alcohols under benign reaction conditions with 100% selectivity and high conversion efficiency with no significant loss in its catalytic activity for 6 cycles [101].

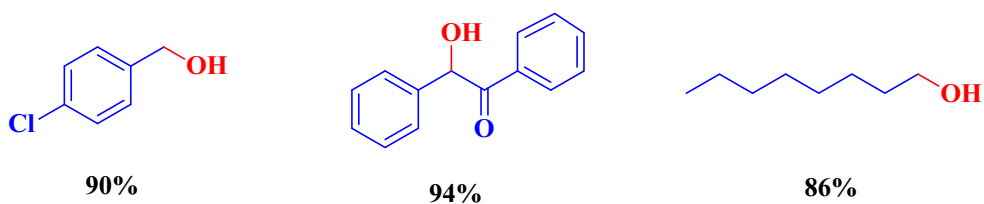
### CDs for oxidative coupling

Anurag Kumar et al. in 2018 demonstrated CDs/Cu<sub>2</sub>O heterogeneous nanocomposite as an excellent catalyst in the coupling of amines 37–38 by photo-oxidation (Scheme 20). To optimize the reaction condition, several solvents have been employed; out of those, acetonitrile conferred better conversion efficiency of 97.5% at 50 °C with 13.9 TON and 1.7 TOF (h<sup>-1</sup>). Having this optimized condition, oxidative coupling of distinct benzylamine substrates under visible light irradiation has been carried out, provided promising yields and best conversion efficiency were observed [102].

Qin Wang et al. in 2020 investigated the use of single atom cobalt catalyst incorporated in CDs as a photocatalyst (CoSAC@CDs) in the coupling of

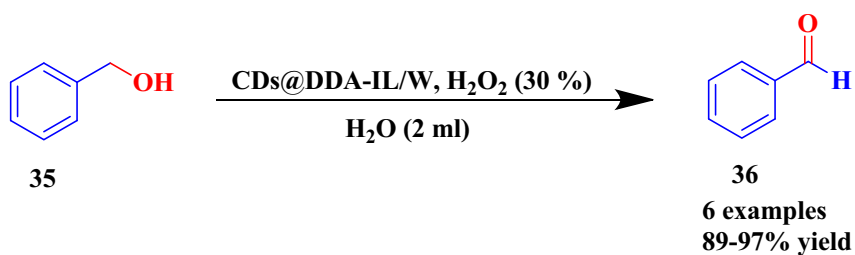


#### Selected substrates

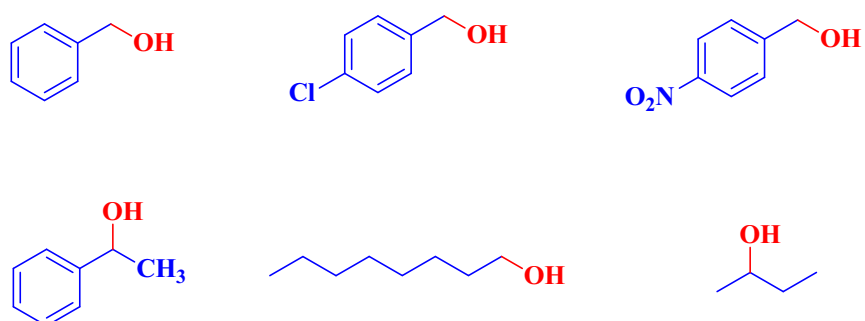


**Scheme 18** CDs@IL/WO<sub>4</sub><sup>2-</sup> catalyzed oxidation of benzyl alcohol.

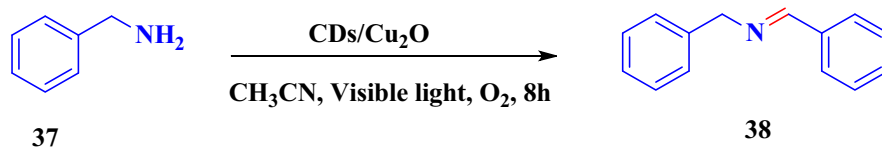
**Scheme 19** CDs@DDA-IL/W catalyzed oxidation of benzyl alcohol.



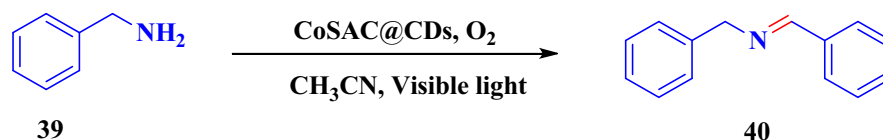
#### Reactants



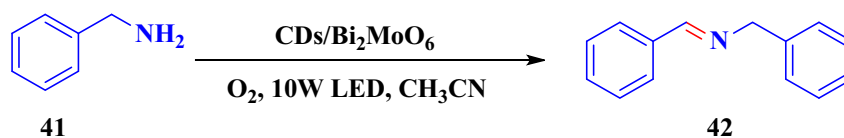
**Scheme 20** Oxidative coupling of benzyl amines using CDs/Cu<sub>2</sub>O nanocomposite.



**Scheme 21** CoSAC@CDs catalyzed oxidative coupling of benzylamines.



**Scheme 22** CDs/Bi<sub>2</sub>MoO<sub>6</sub> catalyzed oxidative coupling of benzylamines.



amines 39 to their corresponding imines 40 by oxidation upon visible light irradiation (Scheme 21). Oxidation of different benzylamine substrates, secondary imines like 1,2,3,4-tetrahydroquinoline, and heterocyclic amines like thiophene-2-ylmethanamine in the presence of O<sub>2</sub> treated with acetonitrile as a solvent was carried out under visible light. The results showed that better conversion efficiency of 99% and good selectivity to the products were observed to almost all substrates. No coupling was observed without the use of this photocatalyst and in darkness. In this reaction, CDs were used as excellent support for Co single atom, produced light-harvesting phenomena, and this catalyst promoted photo-generation and transfer of electron–hole pairs enhancing the catalytic efficiency and served as a promising heterogeneous catalyst [103].

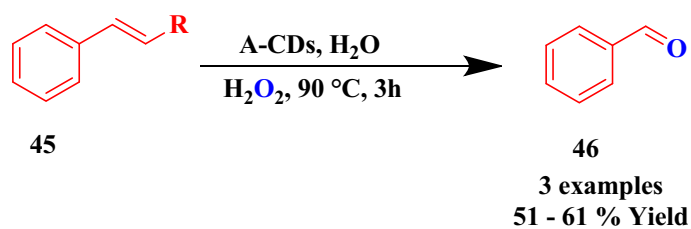
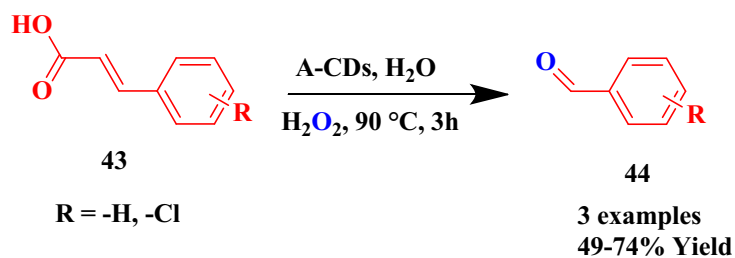
Ye et al. in 2017 presented oxygen-rich CDs as a metal-free carbocatalyst for coupling reaction of benzylamine to N-benzylidene benzylamine by oxidation and the conversion of different alcohols. Comparative performance of different catalysts such as O-CDs, GO, multi-walled carbon nanotubes, HO-CDs, porous GO, and Au/Al<sub>2</sub>O<sub>3</sub> has been reported. In summary, the catalytic and photocatalytic activity of O-CDs was superior to doped carbon catalysts, porous GO, or metal catalysts. Also, oxidation of diverse amines using O-CDs nanocatalyst have been reported. It had been noted that benzylamine containing electron-withdrawing groups such as 4-chlorobenzylamine, provided the highest imine yield of 91%. This facilitation of amine conversion was attributed to the synergism of CDs at the edges of carboxylic groups with unpaired electrons to trap and activate amine and molecular oxygen. This mild procedure of synthesis is utilized in metal-free catalysis for solvent-free oxidations [104].

Subhajyoti Samanta and team in 2017 prepared CDs/Bi<sub>2</sub>MoO<sub>6</sub> nanocomposite as photocatalyst by embedding carbon dots onto the nanoplates of Bi<sub>2</sub>MoO<sub>6</sub> to examine its photocatalytic activity in the coupling of amines. Initially, the optimized condition was found out by choosing the coupling of benzylamine 41 to N-benzylidene benzylamine 42 as the model reaction (Scheme 22) and it was noted that 2.4 wt% of the catalyst, 10 W LED as light source, acetonitrile as a solvent in the presence of oxygen conferred best benzylamine conversion of 84% and imine selectivity to 99%. Having this optimized reaction condition, the coupling of distinct benzylamine substrates by oxidation was carried out and proceeded well [96].

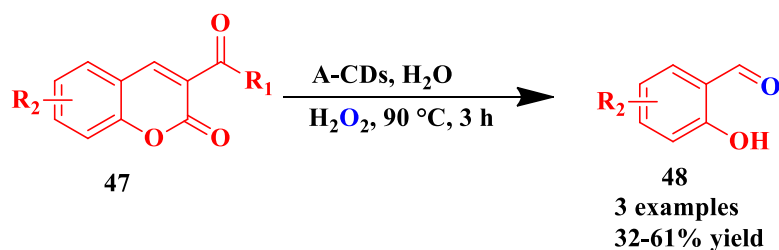
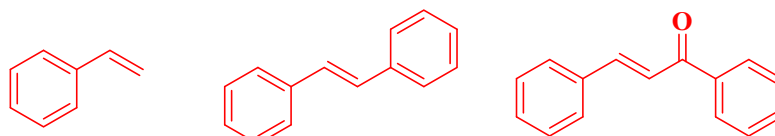
### CDs for oxidative cleavage

In 2020, Dehkordi et al. used amphiphilic CDs integrated with 1-aminopropyl-3-methyl-imidazolium chloride and stearic acid to investigate oxidative cleavage of several olefins which was reported for the first time to their corresponding aldehydes. The main goal for designing this pseudo homogeneous catalyst was to use green solvents such as water in organic reactions without the use of any additives, phase transfer catalyst, or organic solvents. The scope of the designed catalyst was investigated by carrying out oxidative cleavage of cinnamic acid derivatives in the presence of hydrogen peroxide as an oxidant at 90 °C for 3 h. It had been observed that cinnamic acid 43 oxidized to benzaldehyde 44 with a high yield of 74%, while cinnamic acid-containing electron-withdrawing –Cl substituent at para and meta positions gave comparatively less yields of 58% and 49%, respectively (Scheme 23a).

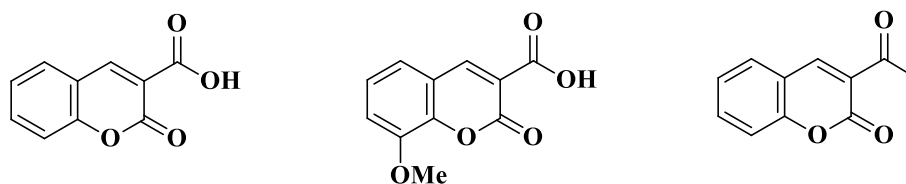
**Scheme 23** a A-CDs catalyzed oxidative cleavage of cinnamic acid derivatives. **b** A-CDs catalyzed oxidative cleavage of multi-substituted alkenes. **c** A-CDs catalyzed oxidative cleavage of derivatives of coumarin-3-carboxylic acid.



Substrates

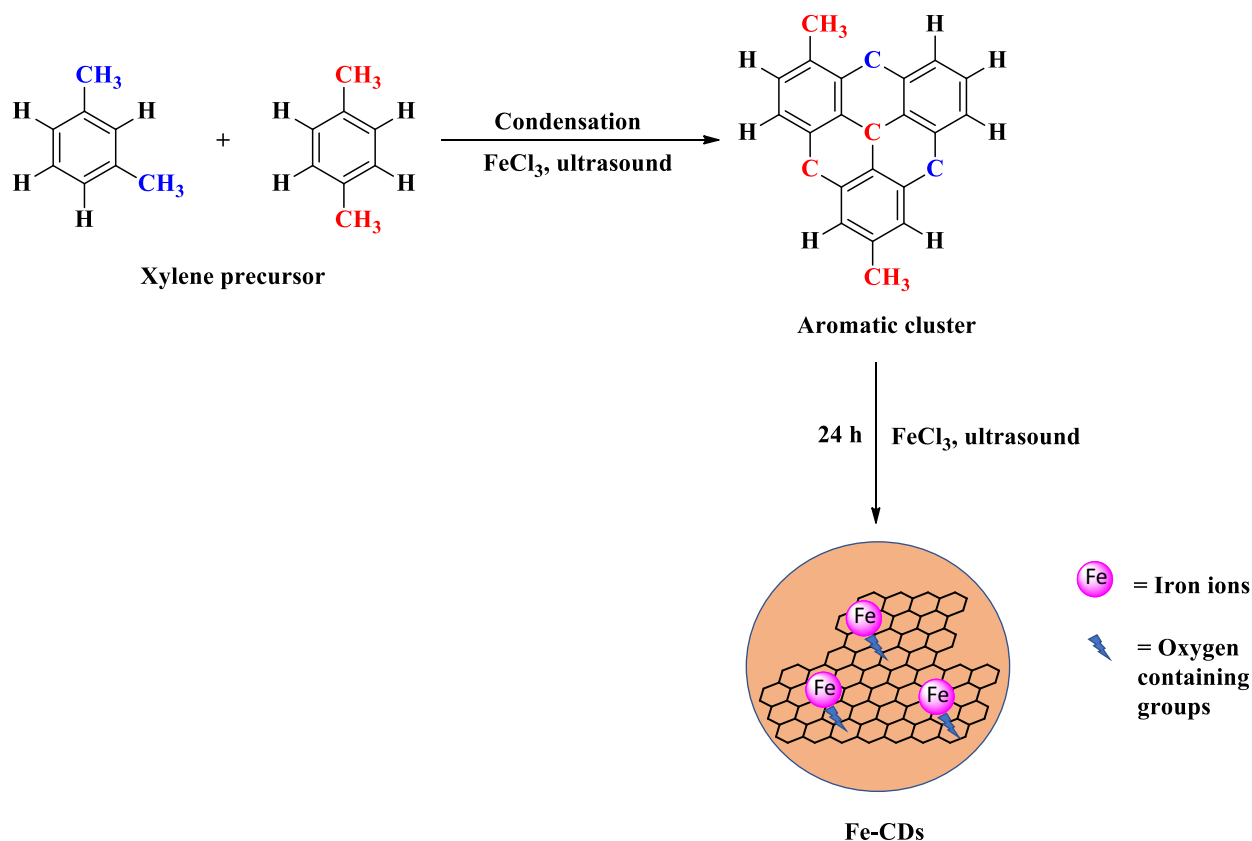


Substrates



Furthermore, the same catalyst was examined in the oxidative cleavage of multi-substituted alkenes 45. The results showed that oxidation of styrene yields benzaldehyde 46 with 57% yield and the

oxidation of trans-stilbene yields benzaldehyde with a 61% yield. In addition to this, oxidation of chalcone yields benzaldehyde with a 51% yield (Scheme 23b).



**Scheme 24** Synthesis of CDs by sonication of xylenes.

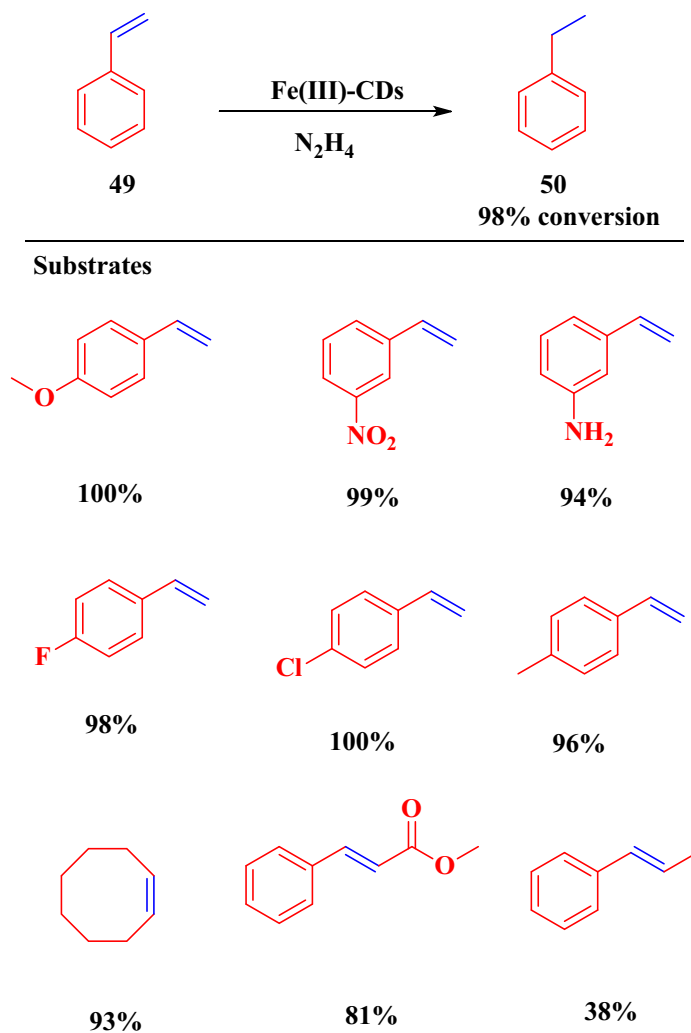
The catalytic efficiency of A-CDs was examined in the selective oxidative cleavage of more stable and non-reactive alkene such as coumarin-3-carboxylic acid derivatives 47 to corresponding product 48. It had been noted that coumarin-3-carboxylic acid oxidized to salicylaldehyde with a 61% yield, and 8-methoxy-2-oxo-2H-chromene-3-carboxylic acid oxidized to ortho-vanillin with 48% yield, while 3-acetylcoumarin yields corresponding oxidative cleavage product with 32% yield (Scheme 23c). In this, it had been observed that C=C cleavage is accompanied by the C-O bond cleavage to produce salicylaldehyde selectively.

The specificity of these A-CDs was that the existence of various hydrophilic and hydrophobic alkyl groups on the CDs surface played an important aspect in bringing hydrogen peroxide and alkenes with a preferred position to reach each other without the need for a phase transfer catalyst. Furthermore, the catalyst can be separated and recycled for up to six runs with no significant reduction in catalytic efficiency [105].

### CDs for reduction reactions

Bourlinos et al. in 2017 achieved the first bottom-up framework for producing Fe(III)-CDs (iron is functionalized on carbon dots) via one-pot oxidative coupling of xylenes by sonication in presence of anhydrous FeCl<sub>3</sub> (Scheme 24). The CDs are spherical, 3–8 nm in size, and are highly dispersible in organic solvents and exhibit PL dependent upon the wavelength. The Fe(III)-CDs were utilized as a heterogeneous photoredox catalyst in the reduction of olefins 49 to corresponding reduced products 50 in the presence of hydrazine as a reducing agent and the decomposition of H<sub>2</sub>O<sub>2</sub> (Scheme 25). Having optimized conditions, reduction of distinct styrene substrates, cyclooctene, methyl-3-phenylpropionate, and  $\beta$ -methyl styrene has been carried out produced better to moderate conversion efficiencies. The Fe(III) ions affixed to the interface of the CDs exhibit exceptional catalytic performance for olefin hydrogenation, with great selectivity and conversion rates up to 100%. Fe(III)-CDs are more powerful in the

**Scheme 25** Hydrogenation of Olefins using Fe(III)-CDs.

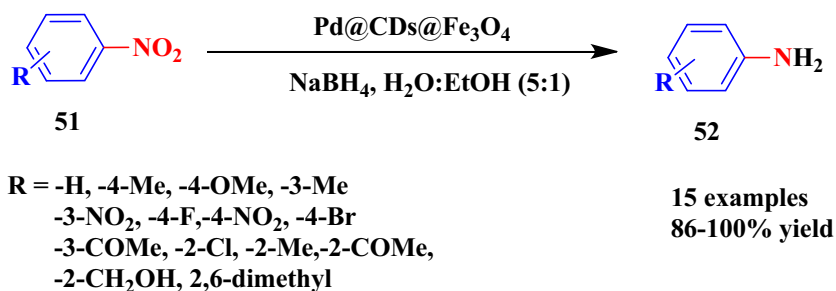


hydrogenation of a series of electron-deficient or electron-donating olefin substrates than typical homogeneous/heterogeneous Fe(III)-based CDs. The enhancement in the catalytic efficiency of this catalyst was ascribed to the dispersion of iron uniformly on the surface. This heterogeneous nanocatalyst can be utilized multiple times without losing its photocatalytic action. Significantly, the constancy of this novel catalyst can be effortlessly evaluated via measurements of quantum yield or PL intensity, allowing for live monitoring in a multitude of scenarios. Fe-CDs were further studied in disintegrating the  $\text{H}_2\text{O}_2$  into water and showed the different catalytic characteristics of these hybrid structures and first-order rate constants of  $0.7 \times 2 \text{ min}^{-1}$  [106].

Gholinejad et al. in 2017 focused on aromatic nitro compounds using the catalyst  $\text{Pd@CDs@Fe}_3\text{O}_4$ . In this method, the CDs were prepared from glycerol

and urea in a green manner. The author reported the best-optimized reaction condition for the reduction of nitroarenes was the use of sodium borohydride as a reducing agent and 0.1 mol% of Pd catalyst which gave 100% conversion efficiency for nitrobenzene 51 to aniline 52 at room temperature (Scheme 26). Furthermore, the efficacy of the reduction of structurally different nitroarenes had been made. From this examination, we came to know that reactions of nitroarenes containing both electron-donating and electron-withdrawing groups proceeded in a good manner and when increasing the reaction time to 4 h for the reduction of p-Me and some substituted nitrobenzene and 12 h for 4-nitroaniline, the maximum yield of 100% was observed and also sterically hindered 2,6-dimethylnitrobenzene reduced to the corresponding product with 91% yield after 24 h. The authors reported that this magnetic catalyst can be

**Scheme 26** Reduction of nitroarenes using  $\text{NaBH}_4$  catalyzed by  $\text{Pd@CDs@Fe}_3\text{O}_4$ .



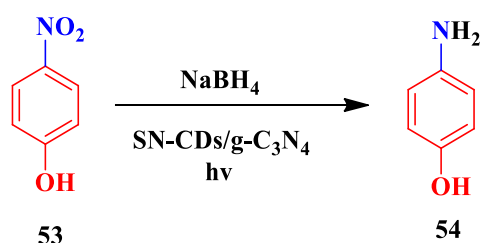
easily separated for more cycles with no significant loss in catalytic activity particularly 7 cycles for the reduction of 4-nitrotoluene [52].

Chang et al. in 2018 developed SN-CDs/ $g\text{-C}_3\text{N}_4$  composite as a novel photocatalyst by incorporating sulfur (S) and nitrogen (N) immobilized carbon dots (SN-CDs) over 2D  $g\text{-C}_3\text{N}_4$  nanosheets. The developed composite was reported to have excellent visible light absorption properties when compared to SN-CDs and  $g\text{-C}_3\text{N}_4$  alone. Better photocatalytic activities of these different catalysts were evaluated by testing them in the 4-nitrophenol 53 to 4-aminophenol 54 photocatalytic reduction reaction in the presence of  $\text{NaBH}_4$  as a reducing agent (Scheme 27). This conversion reaction was carried out with no catalyst or without irradiation of light. The results of this experiment showed that no conversion was observed without catalyst/irradiation of light. However, reduction efficiency of 10% and 50% was achieved, respectively, by the use of individual assistance of SN-CDs and nanosheets of  $g\text{-C}_3\text{N}_4$  as photocatalysts. But a significant reduction of 4-nitrophenol was observed by the use of SN-CDs/ $g\text{-C}_3\text{N}_4$  composite. This could be ascribed to the introduction of more active positions by co-doping with nitrogen and sulfur to carbon dots which makes fine interfacial bonding between  $g\text{-C}_3\text{N}_4$  and SN-CDs. Thus, on visible light irradiation, the photogenerated electrons-hole pairs separated effectively and further

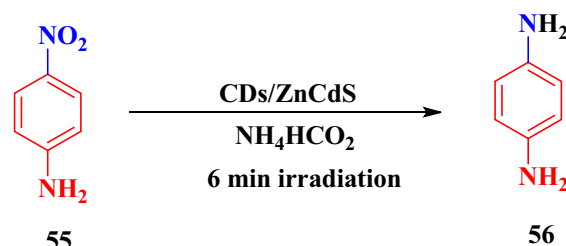
recombination was greatly limited. As a result, the composite enhanced the photocatalytic reduction of 4-nitrophenol [107].

Chai et al. in 2018 carried out the reduction reaction of 4-nitroaniline 55 to p-phenylenediamine 56 by newly designed CDs/ $\text{Zn}^{2+}$  ions doped with cadmium sulfide nanowires (ZnCdS NWs) composite as a photocatalyst (Scheme 28). It had been reported that nearly 100% selectivity of the reaction was observed with the use of ammonium formate as a reducing agent under visible light illumination of  $\lambda > 420$  nm for 6 min. Further, no conversion was observed on prolonged irradiation. This greater selectivity was ascribed to the generation of  $\cdot\text{CO}_2^-$  radicals due to ammonium formate which induced reduction during photoirradiation of ZnCdS NWs. This excellent photocatalytic activity was ascribed to the increase in the valence band potential of CdS rather than decreasing the conduction band potential. Furthermore, a decrease in the reduction efficiency of CDs/ZnCdS NWs was observed because of no production of  $\cdot\text{CO}_2^-$  radicals, when 0.05 M of  $\text{Na}_2\text{SO}_3$  and  $\text{Na}_2\text{S}$  were used as hole scavengers instead of ammonium formate. However, the efficient separation of photo-generated carriers was exhibited by CDs as co-catalyst in enhancing the photocatalytic activity of ZnCdS nanowires [108].

Liu and his co-workers in 2019 focused on  $\text{SnS}_2$  2D-layered material as a semiconductor photocatalyst to



**Scheme 27** Photoreduction of 4-nitrophenol using SN-CDs/ $g\text{-C}_3\text{N}_4$ .



**Scheme 28** Photoreduction of 4-nitroaniline to 4-phenylenediamine.

demonstrate its photocatalytic reduction performance on aromatic nitro compounds **57** to corresponding reduced products **58**. However, they have found photogenerated electron–hole pair recombination and active hydrogen got weakly absorbed from  $\text{NaBH}_4$  hydrolysis as an obstacle during the photocatalytic reduction process of semiconductors that greatly suppressed the catalytic efficiency. To attain significant enhancement in the photocatalytic reduction of aromatic nitro compounds, several techniques have been used such as coupling of semiconductors, doping alien atoms, and compositing with noble metals and carbon materials. Out of those,  $\text{CDs@Pd}$  nanoclusters conferred excellent chemical stability, in situ reductions of  $\text{Pd(II)}$ , and showed a fast and efficient transfer of photogenerated electrons when it was attached with  $\text{SnS}_2$  nanosheets through strong bonding sulfur ions on the nanometric surface of Pd. The synthesized composite was used to efficiently reduce various aromatic nitro compounds under visible light in  $\text{H}_2\text{O}$  and  $\text{NaBH}_4$ . A comparative study had been made to see the efficient catalytic activity of pure  $\text{SnS}_2$ ,  $\text{CDs-SnS}_2$ ,  $\text{Pd-SnS}_2$ , and  $\text{CDs@Pd-SnS}_2$  on the reduction of **75**. From these catalysts, the  $\text{CDs@Pd-SnS}_2$  composite exhibited a higher conversion rate of 99.7% under visible light irradiation for 40 min (Scheme 29) and 41.1% in dark. A lower conversion rate of 5.3% reduction had been reported for the  $\text{Pd-SnS}_2$  catalyst without CDs. This could be attributed that smaller  $\text{CDs@Pd}$  (< 5 nm) promoted strong active hydrogen absorption and fast transfer of electrons on  $\text{CDs@Pd-SnS}_2$ . Furthermore, due to the stabilization of Pd nanoparticles by CDs on  $\text{SnS}_2$  nanoparticles, it had been observed that there is no deterioration of catalytic activity of the designed catalyst for four cyclic runs [109].

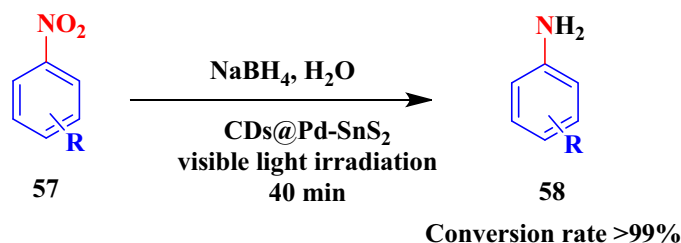
Amadio and group in 2020 described the use of nitrogen-doped carbon dots (N-CDs) in the picolinium esters **59** photocleavage reduction to afford N-methyl-4-methylpyridinium **60** and the respective carboxylic acids **61** (Scheme 30) with higher

conversion and selectivity up to 99% within 48 h of reaction time in a solvent such as deuterated acetonitrile and water mixture in nitrogen environment upon 365 nm UV irradiation. In this reaction, EDTA acted as a sacrificial donor of electrons upon using low N-CDs catalyst loading of 20 mg/mL, but it was not required upon high catalyst loading. No reaction was found without catalyst or light ensured requirement of both the components, and also, the recyclability of the catalyst was not attempted there [110].

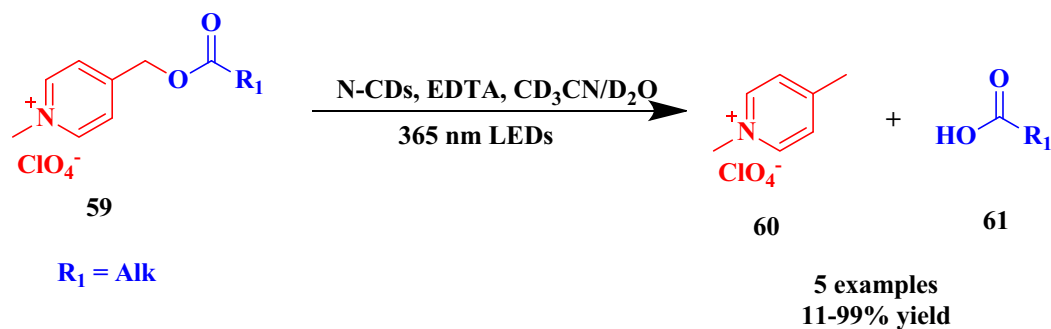
### CDs for hydrogenation reactions

Sadjadi et al. in 2019 constructed a ternary hybrid system comprising of  $\text{Pd@magnetic CDs}$  incorporated in a 3D-polymeric network of cyclodextrin nanosponges (CDNS) and biochar prepared from Bell-pepper for the first time as a heterogeneous catalyst which was used in the hydrogenation of nitroarenes. To test the selectivity and efficiency of the catalyst, hydrogenation of different nitroarenes **62** to corresponding hydrogenated products **63** has been reported (Scheme 31). Out of those, nitrobenzene gave an excellent yield of 100%. Hydrogenation of 4-nitroacetophenone and 4-nitroaniline also afforded the corresponding products in high yield but comparatively lower than that of nitrobenzene. As far as the reaction with 1-nitronaphthalene and 1-bromonitrobenzene was concerned, comparatively fewer yields of 80% and 55%, respectively, were observed. This could be attributed to the encapsulation of these bulky molecules inside the cavities of CDNS which was difficult, as these molecules have substituents ortho to each other. To investigate the catalytic efficiency of the catalyst, hydrogenation of nitrobenzene with  $\text{Pd@CDs@Fe}$  alone and that with hybrid, biochar, and CDNS were performed. Out of those,  $\text{Pd@CDs@Fe/hybrid}$  gave an excellent yield of 100%, whereas  $\text{Pd@CDs@Fe/CDNS}$  gave a low yield of 75%. These results indicated that the contribution

**Scheme 29** Photoreduction of aromatic nitro compounds using  $\text{CDs@Pd-SnS}_2$ .

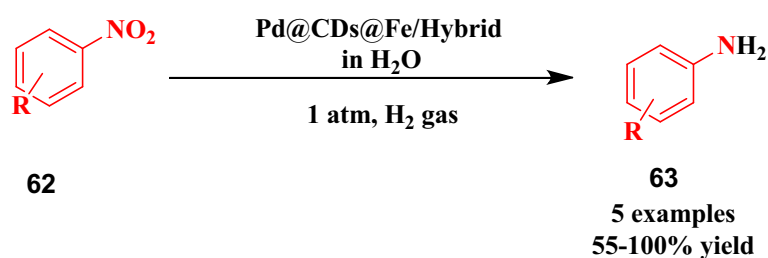




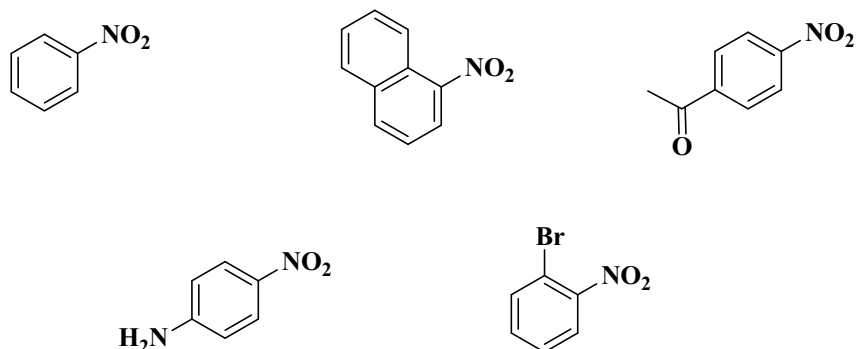


**Scheme 30** N-CDs catalyzed reductive photocleavage reactions.

**Scheme 31** Hydrogenation of nitroarenes catalyzed by Pd@CDs@Fe/Hybrid.



#### Substrates



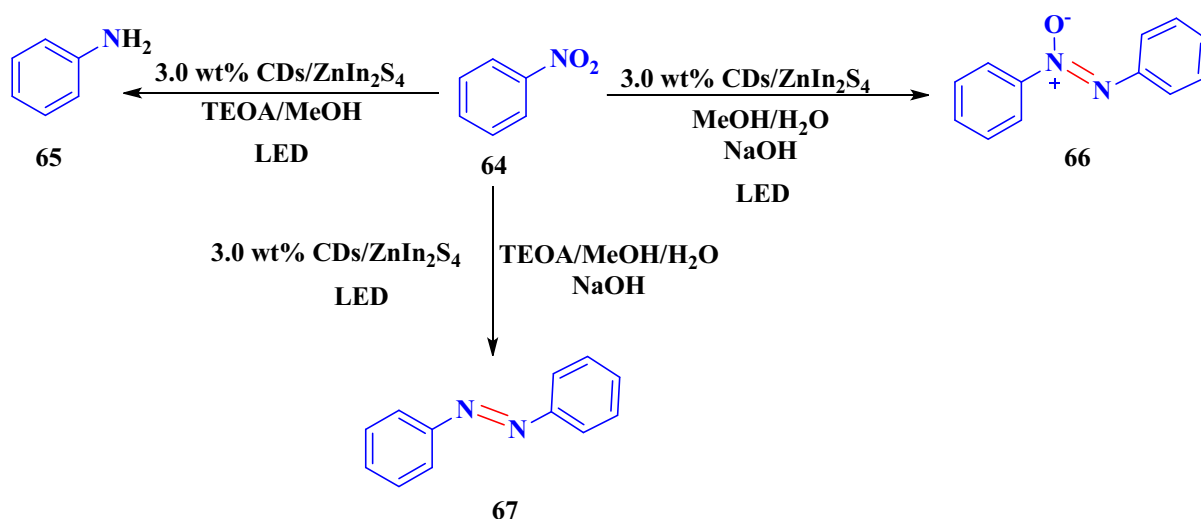
of each component was important in enhancing the catalytic activity. Moreover, the recyclability and recovery of the catalyst were easy due to the magnetic property of the catalyst [111].

To improve green and sustainable organic synthetic methods, many interests had been paid to photoredox reactions in which visible light was used to trigger organic transformations under mild reaction conditions. In continuation with this idea, Wang et al. in 2020 developed the successful synthesis of aniline 65, azoxybenzene 66, and azobenzene 67 by simply controlling the medium of the reaction in the photocatalytic hydrogenation of nitrobenzene 64 (Scheme 32) using CDs/ZnIn<sub>2</sub>S<sub>4</sub> nanocomposite (3.0 wt%) as a photocatalyst which is free from noble metals. The solvents employed in the conversions of

64–65, 66, and 67 were triethanolamine/methanol (TEOA/MeOH), MeOH/H<sub>2</sub>O, and TEOA/MeOH/H<sub>2</sub>O, respectively, and the base used was NaOH for the conversions of 64–66 and 67. The CDs/ZnIn<sub>2</sub>S<sub>4</sub> nanocomposite was formed by the self-assembly of ZnIn<sub>2</sub>S<sub>4</sub> in CDs, which was reliant on the medium of the reaction and hydrogen power source [112].

#### CDs in multi-component synthesis

Mayank et al. in 2017 demonstrated a new alternative protocol as a green method for the multi-component reaction to synthesize 4H-chromene derivatives 71 and 72 by employing 1-naphthol or 2-naphthol 68, 4-hydroxy benzaldehyde 69, and malononitrile 70 as reactants using the sonication method. On behalf of

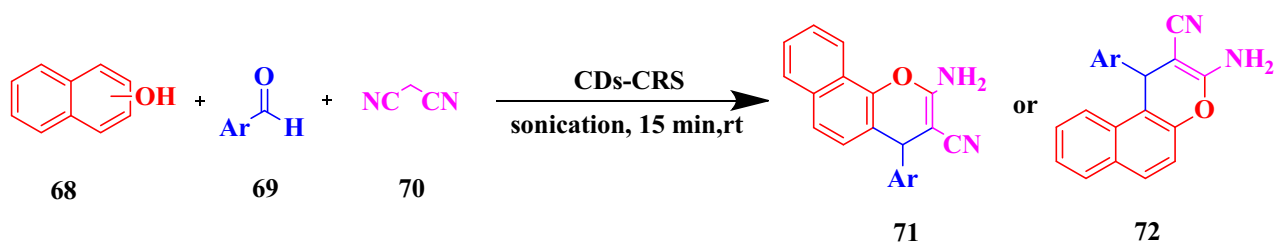


**Scheme 32** CDs/ZnIn<sub>2</sub>S<sub>4</sub> catalyzed chemoselective hydrogenation under light irradiation.

unique structure, H-bonding interactions, trans-phase, and polarity, water was chosen as solvent. But the poor solubilizing ability of water toward organic reactants and ionic liquids was introduced to solvate the organic reactants to form micelles. In this reaction, CDs were used as a catalyst for their non-toxic nature, high stability, environmentally friendly composition, and reusability and also used to activate the carbonyl group of aldehyde to accelerate the condensation. In this, the CDs were obtained from pyrolysis of aqueous citric acid for 6 h at 160 °C followed by centrifugation and dialysis against water. The ionic liquid (IL) formed micelles with CDs to give a CDs-CRS due to its self-assembling nature that could give multiple variants if changing the components of the ILs/CDs. They reported a series of experiments using CDs-CRS, CDs, IL-1(1-Methyl-3-octyl-1H-imidazol-3-ium), and IL-2(3-dodecyl-1-methyl-1H-imidazol-3-ium) alone, to test their efficiency toward 4H-chromene derivatives synthesis. Out of those, CDs-CRS with IL-2 (3-dodecyl-1-methyl-1H-imidazol-3-ium) gave a better yield of 98% concerning reaction time (15 min), temperature (20–40 °C), and above critical micelle concentration (Scheme 33). This could be attributed to the trapping capacity of the IL-2 which was more than that of IL-1 because it contained a long side chain in which the reactants and CDs could be easily trapped inside it. Hence, the reaction proceeded more smoothly. Also, structurally different aldehydes do not alter the reaction so far. Moreover, it was seen that temperature more than 40 °C disrupts the structure of the

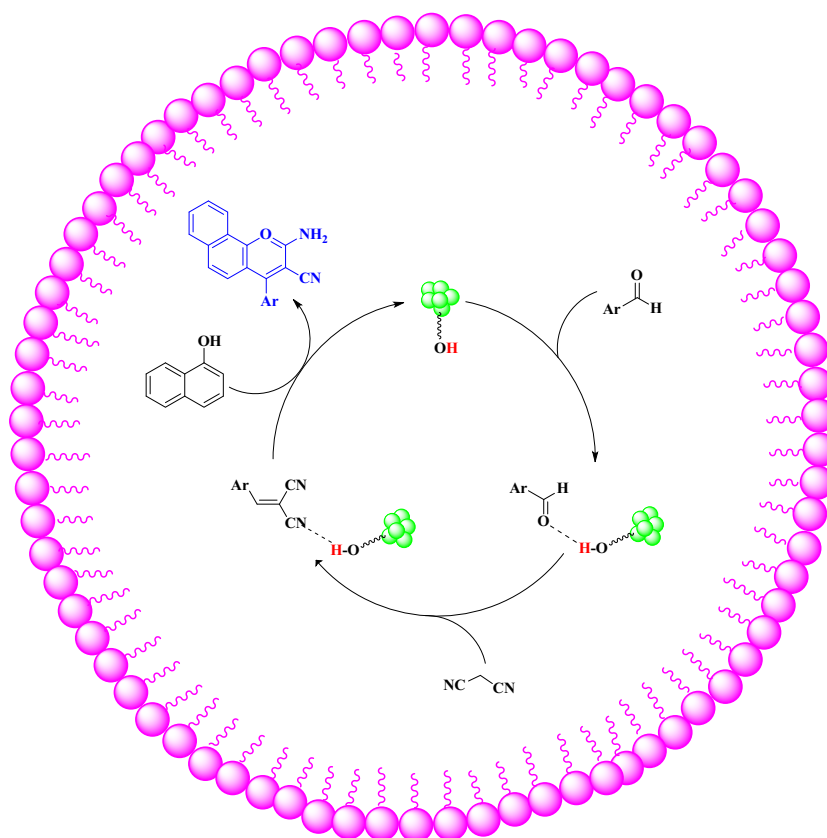
micelle and the products' yield got affected. The suggested mechanism was illustrated in (Scheme 33a) where the organic reactant molecule accumulates into the micelles' cavity owing to their hydrophobic nature. Then, CDs activate the carbonyl group of benzaldehyde via hydrogen bonding due to the presence of polar groups on the surface of CDs, thereby accelerating the condensation by nucleophilic attack of malononitrile. Further activation drives the condensation resulting in corresponding 4H-chromene derivatives. The catalyst recyclability was tested by concentrating the filtrate to the original volume to attain CMC concentration, with that the further reaction was carried out with 1-naphthol, 4-hydroxy benzaldehyde, and malononitrile and it was found that the efficacy of the catalyst remained the same for over ten runs [113].

Narayanan and his co-workers in 2018 synthesized sulfonated coconut shell char incorporated with carbon dots as a catalyst (SCSC) in the synthesis of amidoalkyl naphthols. Among different sulfonated CSC, the best catalyst was found by taking model reaction in the synthesis of N-[Phenyl-(2-hydroxy-naphthalen-1yl)-methyl]-benzamide 76 using benzaldehyde 73,  $\beta$ -naphthol 74, and benzamide 75 as starting materials at 125 °C in a solvent-free environment. The use of SCSC30 (30 g sulfuric acid to sulfonate 1 g of CSC) as a catalyst in this reaction afforded 98% yield within 3 min of reaction time (Scheme 34). Moreover, the catalyst application was extended in the synthesis of distinct amidoalkyl naphthols which afforded better product yields. The



Ar = -C<sub>6</sub>H<sub>5</sub>, -3-HO-C<sub>6</sub>H<sub>4</sub>, -2-HO-C<sub>6</sub>H<sub>4</sub>, -4-MeO-C<sub>6</sub>H<sub>4</sub>,  
 -3-MeO-C<sub>6</sub>H<sub>4</sub>, -3,4-(MeO)<sub>2</sub>C<sub>6</sub>H<sub>3</sub>, -2,5-(MeO)<sub>2</sub>C<sub>6</sub>H<sub>3</sub>,  
 -2,3,4-(MeO)<sub>3</sub>C<sub>6</sub>H<sub>2</sub>, -4-F-C<sub>6</sub>H<sub>4</sub>, -2-Cl-C<sub>6</sub>H<sub>4</sub>, -4-Cl-C<sub>6</sub>H<sub>4</sub>

11 examples  
 with IL-1 95 to 98% yield  
 with IL-2 97-99% yield



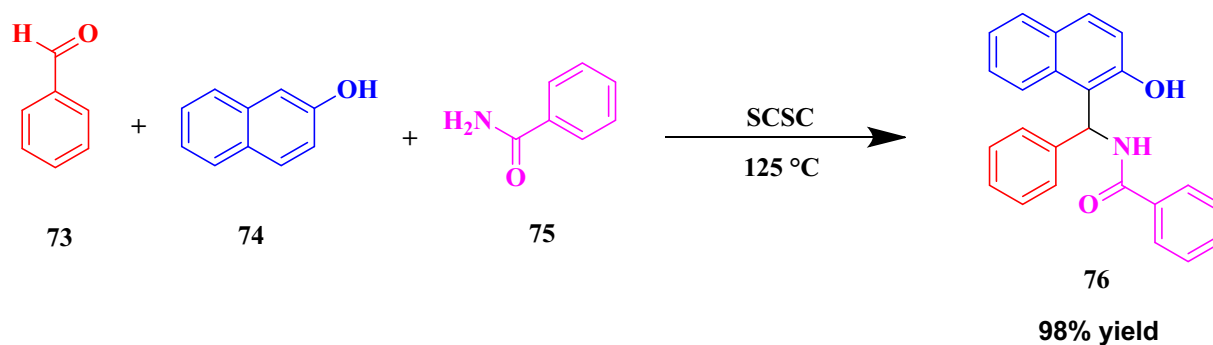
**Scheme 33** Synthesis of 4H-chromene derivatives using CDs-CRS. **a** Proposed mechanism for the synthesis of 4H-chromene using CDs-CRS.

reported catalyst ensured heterogeneity and recyclability and can be reused up to 6 runs with a minimum 7% loss in the product yield [114].

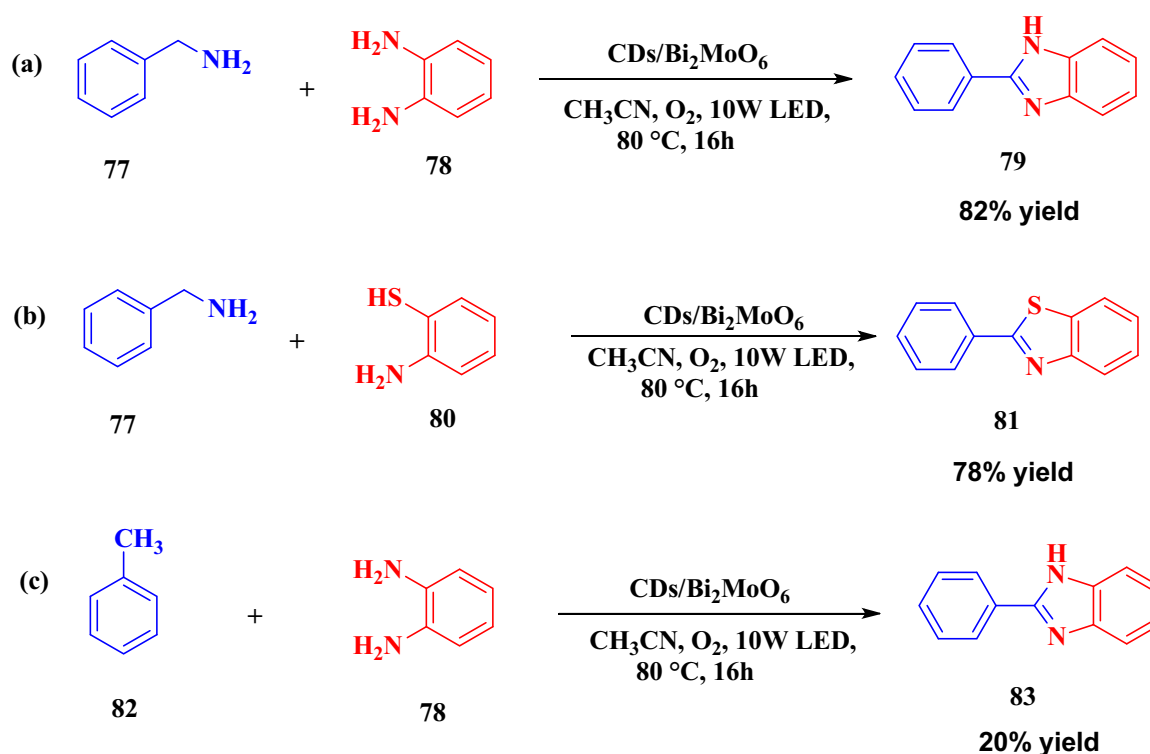
### CDs for heterocycle synthesis

Subhajyoti Samanta and team in 2017 prepared CDs/Bi<sub>2</sub>MoO<sub>6</sub> nanocomposite as photocatalyst by embedding carbon dots onto the nanoplates of Bi<sub>2</sub>MoO<sub>6</sub> to examine its photocatalytic activity in one-pot

heterocyclic synthesis under the optimized condition of 2.4 wt% of the catalyst, 10 W LED as light source, acetonitrile as a solvent in the presence of oxygen. In this, the catalyst was checked to synthesize benzimidazole 79 by the one-pot reaction between benzylamine 77 and *o*-phenylenediamine 78 which gave 82% yield. In addition to this, benzothiazole 81 was synthesized by reacting benzylamine 77 and *o*-aminothiophenol 80 as starting materials which



**Scheme 34** Synthesis of amidoalkyl naphthol catalyzed sulfonated coconut shell char.



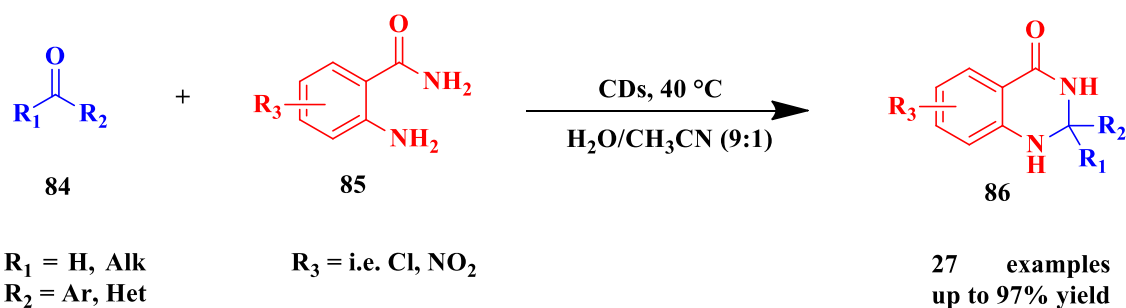
**Scheme 35** CDs/Bi<sub>2</sub>MoO<sub>6</sub> catalyzed synthesis of benzimidazole and benzothiazole.

gave a good yield of 78%. Benzimidazole was also prepared using the same catalyst by toluene 82 as starting material instead of using benzylamine, but only a 20% yield of 83 was observed (Scheme 35) with a 6% benzaldehyde side product [96].

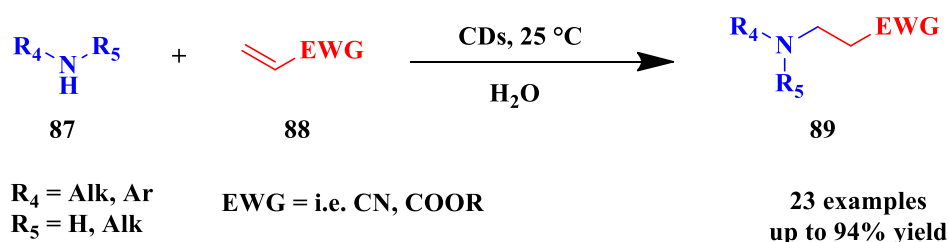
Sarma et al., in 2017 utilized the carboxyl functionalized carbon nanodots (CNDs) in the glyco/spiro/dihydro quinazolinones synthesis and the formation of aza-Michael adducts. Firstly, the authors reported the use of these CNDs in catalyzing the condensation between carbonyl compounds 84 and 2-aminobenzamide derivatives 85 in the presence of a solvent such as water/acetonitrile to give the

corresponding quinazolinone derivatives 86 at 40 °C with a catalyst loading of 0.5 mg/mL (Scheme 36a). Then, the same catalyst was employed in the aza-Michael reaction of amines 87 and  $\alpha$ ,  $\beta$ -unsaturated compounds 88 with the electron-deficient center to give aza-Michael adduct 89 in water with a very good yield up to 94% at room temperature with the same catalyst loading (Scheme 36b). For both the transformations, the reusability of the catalyst remained moreover same for three cycles and can be recycled by simple extraction workup [115].

Majumdar et al. in 2018 developed a novel protocol to synthesize quinazolinone derivatives as a one-pot



(a)



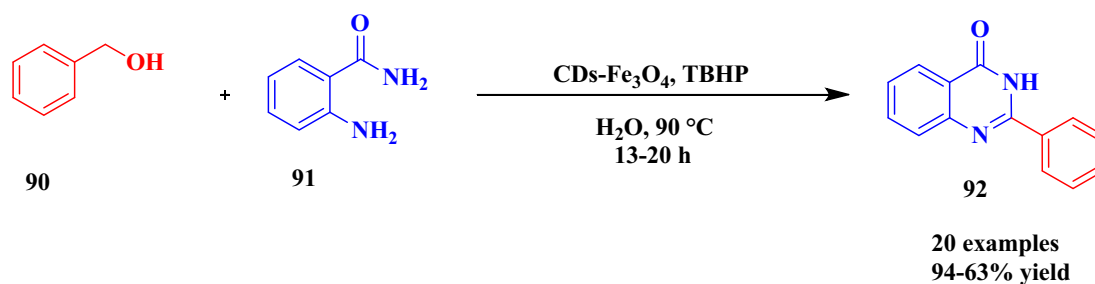
(b)

**Scheme 36** a CDs catalyzed cyclo-condensation reaction. b CDs catalyzed aza-Michael reaction.

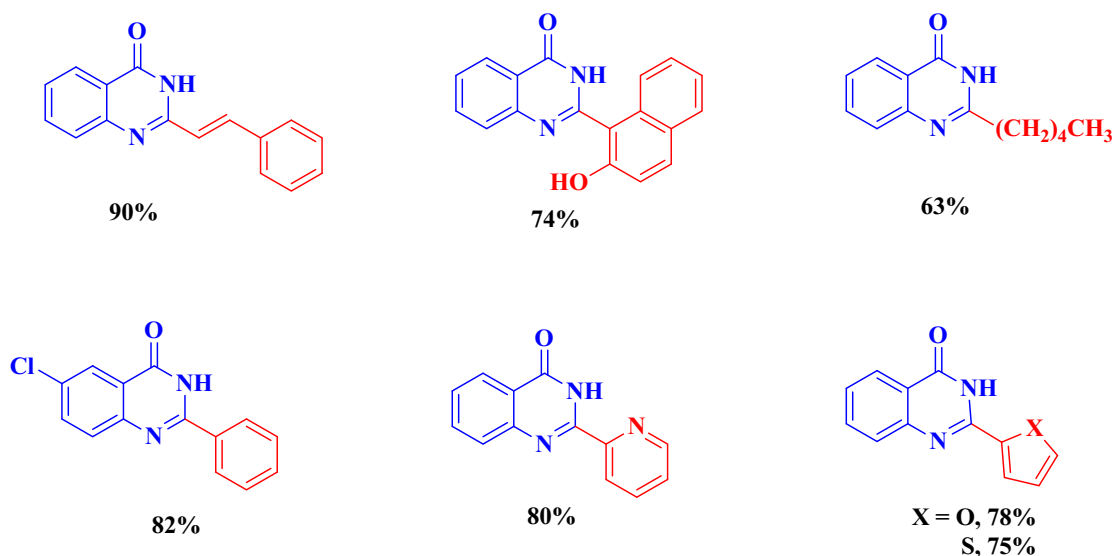
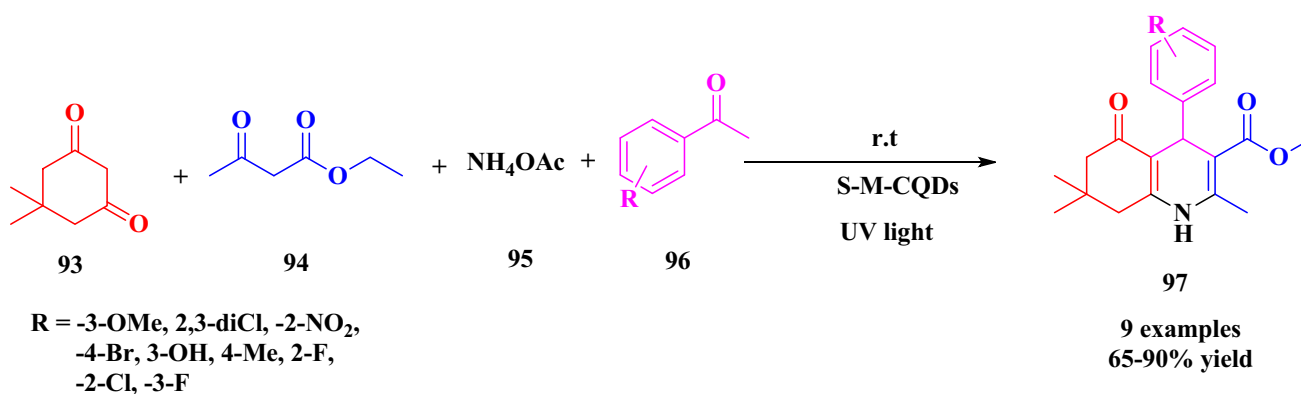
tandem reaction from alcohols 90 and 2-amino benzamide 91 substrates as starting materials in an aqueous medium catalyzed by CDs-Fe<sub>3</sub>O<sub>4</sub> composite. The CDs from this composite were prepared by the microwave treatment of PEG-200. The prepared catalyst provides an excellent yield of quinazolinone derivatives 92 with TBHP as an oxidant (Scheme 37). Because of their intrinsic acidic and oxidative characteristics, CDs also exhibit high carbocatalytic activity for a wide range of chemical reactions. In this, CDs have not only served as an excellent surface-stabilizing agent for the Fe<sub>3</sub>O<sub>4</sub> NPs but also increases composite's catalytic activity via their fundamental peroxidase activity. The scope of the reaction was evaluated under optimal conditions by using 10 wt% Fe<sub>3</sub>O<sub>4</sub>-CND nanocomposites as a catalyst and TBHP as an oxidizer for 16 h in aqueous media at 90 °C. Reactions with benzyl alcohol substrates and bearing electron-releasing as well electron-deficient substituents were well tolerated affording good to excellent yields (94–63% yield). Similarly, reactions with 2-aminobenzamides substrates bearing halo, electron-rich, and poor

substituents gave corresponding products with excellent yields, while the fused ring and aliphatic inactive alcohols also gave fairly good yields. Even though heteroatoms tend to poison the surface of the metal oxide, through this synthetic protocol, the challenging heterocyclic alcohols can be effectively transformed into their corresponding quinazolinone derivatives with high yields. The authors reported that this magnetic catalyst can be retained easily and reused for several cycles with excellent efficiency [116].

Sarmasti et al. in 2019 synthesized hexahydroquinoline derivatives 97 as a one-pot multi-component heterocycle synthesis using dimedon 93, ethyl acetoacetate 94, ammonium acetate 95, and benzaldehyde derivatives 96 as starting materials catalyzed by sulfonated magnetic carbon quantum dots (S-M-CDs or Fe<sub>3</sub>O<sub>4</sub>@CDs-SO<sub>3</sub>H) as a solid photo-switchable acid catalyst under UV light irradiation at room temperature (Scheme 38). At first, the catalytic abilities of different catalysts were examined under dark and on UV light irradiation in the reaction of dimedon, ethyl acetoacetate, ammonium acetate, and



## Selected examples

Scheme 37 Synthesis of quinazolinone derivatives catalyzed by  $\text{Fe}_3\text{O}_4$ -CND composite.

Scheme 38 Synthesis of hexahydroquinoline derivatives.

benzaldehyde. A maximum yield of 75% was observed for S-M-CDs under UV exposure indicating the importance of the sulfonic acid group in the

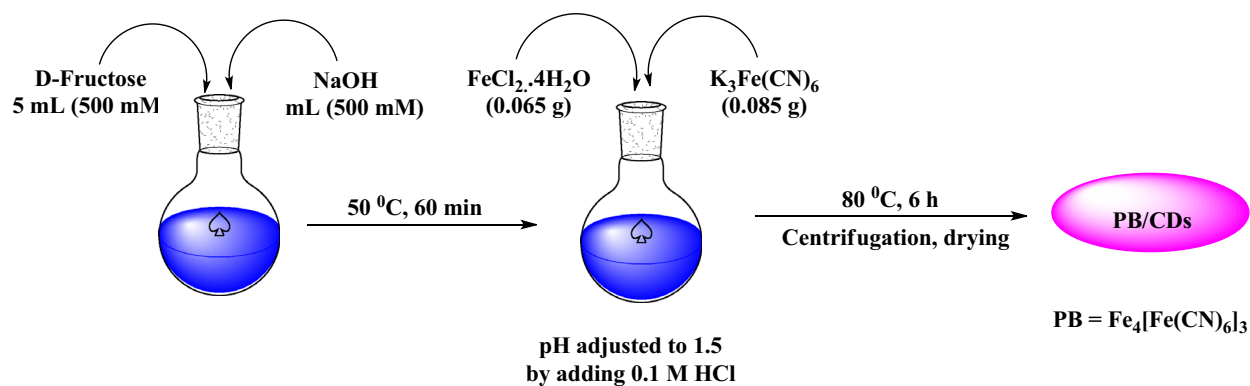
catalyst which generates protons on light irradiation causing an enhancement in the reaction. Different benzaldehyde substrates yield different

hexahydroquinoline derivatives with good to better product yields (65–90%) on UV light irradiation with a lesser reaction time of 10–6 min, whereas in dark obtain 62–87% yields but with longer time to completion of the reaction. The catalyst was reported to be retrieved using a magnet easily and can be used for further reactions [117].

### CDs for C–H activation of amines

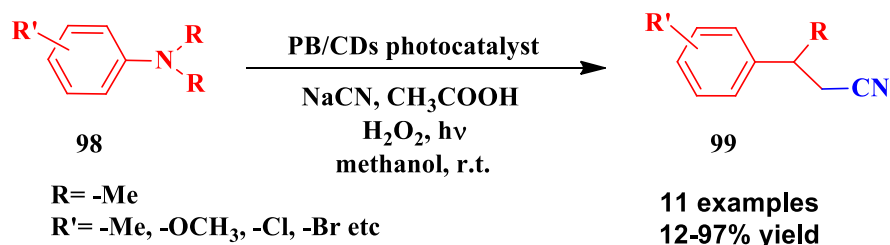
Photoredox catalysis based on visible light is expected to be a useful technique in organic synthesis for a wide variety of chemical transformations. Those reactions make use of visible light, which is both harmless and abundant, as well as sustainable. [118, 119]. The C–H activation of amines is of special importance since the ensuing  $\alpha$ -aminonitriles are the key intermediates in the production of bioactive natural products, artificial  $\alpha$ -amino acids, and heterocyclic compounds [120, 121]. The Strecker reaction between a carbonyl molecule, an amine, and a cyanide is used in the industrial synthesis of  $\alpha$ -aminonitriles [122]. Likewise, for their synthesis, a handful of stoichiometric reagents that normally generate excessive amounts of unwanted waste were utilized. In recent decades, several transition metals-based catalyzed C–H activation of amines has been reported. For this chemical transition, molecular homogeneous photocatalysts based on Ir and Ru have recently been described [123, 124]. Yet, the high expense, toxic, and homogeneous behavior of such catalysts restricts their utility in practical applications. As a result, heterogeneous photocatalysis is regarded to be a promising solution for resolving the non-recyclability of homogeneous catalysts.

Thus, Maaoui et al. in 2016 documented the first literature method to use CDs on Prussian blue (PB) to make nano-photocatalyst for C–H activation of amines. In this, CDs were prepared by alkaline hydrolysis of D-fructose for 60 min at 50 °C, followed by subsequent addition of  $\text{FeCl}_2 \cdot 4\text{H}_2\text{O}$  and  $\text{K}_3\text{Fe}(\text{CN})_6$  to get the desired nanocomposite (Scheme 39). Herein, they have reported the synthesis of  $\alpha$ -aminonitriles 99 from tertiary amines 98 by activating C–H bond with PB/CDs nanocomposite as catalyst under visible light irradiation using methanol as solvent, hydrogen peroxide as oxidant, and NaCN/acetic acid as the source of cyanide (Scheme 40). To study the optimization conditions, the reaction of N, N'-dimethyl aniline was taken. The results indicated that the use of PB/CDs nanocomposite upon light irradiation for 8 h with former mentioned reaction condition afforded maximum yield of 94% with excellent TOF of  $11.7 \text{ h}^{-1}$ , while individual use of PB and CDs and also PB/CDs nanocomposite without light irradiation resulted in no reaction and the use of individual assistance of PB and CDs with light irradiation affords poor yields of 18% and 8%, respectively. This poor efficiency of CDs can be attributed to the photogenerated electron–hole pairs of CDs that can trigger the oxidative cyanation, but the transfer of electrons to the substrates is suppressed due to the limited availability of redox sites. The scope and limitation of this synthesis were tested for the oxidative cyanation of various substituted N, N'-dimethyl anilines. Herein, they have reported 11 examples, out of which p-substituted N, N'-dimethyl anilines were observed to be more reactive than the ortho- and meta-substituted ones. However, no conversion was observed for n-tributylamine and a poor yield of 12% was observed for the benzyl group-



**Scheme 39** Synthesis of PB/CDs nanocomposite.

**Scheme 40** PB/CDs nanocomposites photocatalyzed C-H activation of amines.



containing tertiary amines. Due to the heterogeneity of the PB/CDs photocatalyst, it can be retrieved easily by centrifugation, recycled, and reused for four runs with minimum loss in its photocatalytic activity [125].

### CDs for cycloaddition reaction

The most exquisite example of “click chemistry” is the Huisgen Cu(I)-catalyzed 1,3-dipolar cycloaddition reaction between terminal azides and alkynes (CuAAC), which offers a broad array of applications in organic synthesis, as well as electrochemical and biological applications [126, 127]. Nonetheless, the conventional strategy of generating Cu(I) compounds (monovalent) from Cu(II) salt has difficulty in separation, in the Cu(I) catalyzed “click chemistry,” which has been invented by the groups of Sharpless and Medal [128]. Despite the widespread usage of Cu(I) complexes to catalyze this cycloaddition, the difficulty of Cu(I)-releasing ligands and the manufacture of complicated catalysts tranquil restricts the opportunity of “click chemistry” [129]. An alternative technique is indeed urgently required to eliminate the necessity for a radical initiator or reducing agent [130].

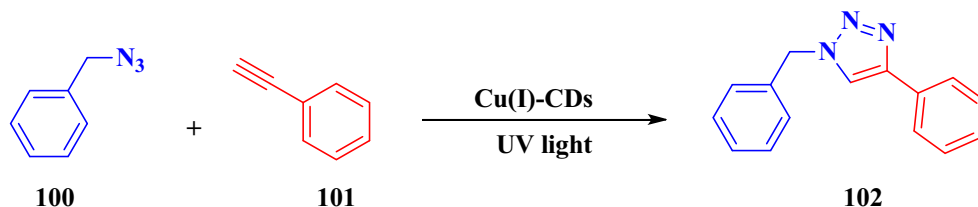
In 2017, Liu and his co-workers concentrated 1,3-dipolar cycloaddition of terminal azides such as benzyl azide 100 and terminal alkyne 101 such as phenylacetylene catalyzed by Cu(I)-doped CDs to give 5-membered heterocycle and 1,4-Diphenyl-1H-1,2,3-triazole 102 (Scheme 41) on UV light irradiation (365 nm). The Cu(I)-doped CDs were prepared by the thermolysis treatment of ascorbic acid and

$\text{Na}_2[\text{Cu}(\text{EDTA})]$  at 250 °C. The Cu(II) was reduced to Cu(I) by ascorbic acid as a reducing agent and provides a higher Cu(I) doping ratio of 1.41%. The use of CDs in this reaction was to provide a new way to “Click Chemistry” by avoiding side reactions with a minimum amount of catalyst loading and for the bio-friendly development of nanocatalysts. These zigzagged CDs allow Cu(I) to reside firmly and to release quickly, compared with conventional catalysts. The UV-induced split of excitons has been examined as a promising option for investigating the plausible mechanism for catalyzing CuAAC reaction. CDs allowed electrons to escape and then finally release Cu(I) from CDs to drive this cycloaddition without the need for utilizing a reducing agent or Cu(II) salts [131].

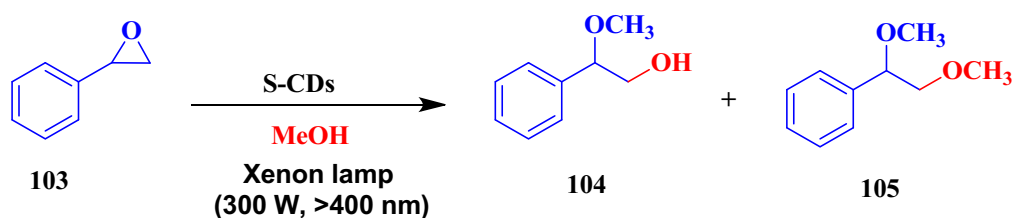
### CDs for ring-opening of epoxides

Li et al. in 2015 investigated the ring-opening of epoxides by acid catalyst (photo-switchable). Hence, they prepared CDs decorated with hydrogen sulfate groups (S-CDs) to catalyze ring-opening of epoxides 103 with methanol and other primary alcohols to the products 104 and 105 (Scheme 42). Electrochemical techniques in pure water were used to make CDs from a graphite rod. The S-CDs were obtained after a reasonable time of reflux treatment in  $\text{H}_2\text{SO}_4$  solution. The CDs' shape (spherical) and size were revealed by TEM pictures (2–9 nm), whereas the FTIR and EDX spectroscopy confirmed the existence of sulfate groups on the surface of the CDs. The reported catalyst exhibited proton-generating ability on visible light irradiation with high conversion

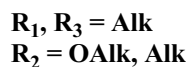
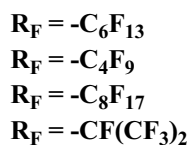
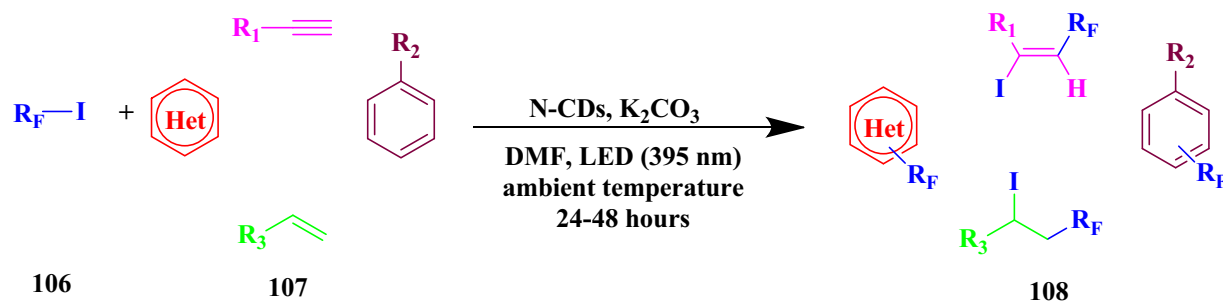
**Scheme 41** Cu(I)-CDs catalyzed Huisgen 1,3-dipolar cycloaddition.





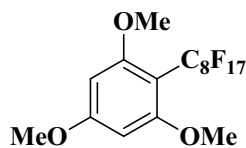


**Scheme 42** Ring-opening of styrene oxide catalyzed by sulfated CDs.

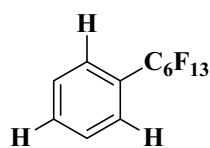


20 examples  
22–93% yield

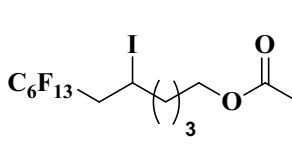
### Selected substrates



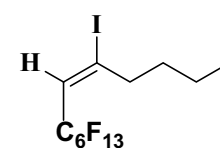
93% yield



22% yield



90% yield



76% yield (E/Z 4:1)

**Scheme 43** N-CDs catalyzed photochemical perfluoroalkylations.

efficiency. The photoexcitation and charge separation in the CDs, which induce an electron-withdrawing force from the acidic groups, are revealed to be the cause of this reversible, light-switchable acidity. The conversion efficiency of the comparative performance of different catalysts such as S-CDs, GO,  $H_2SO_4$ ,  $p\text{-CH}_3\text{-C}_6\text{H}_4\text{-SO}_3\text{H}$ ,  $\text{CH}_3\text{COOH}$ , and Norit A was examined in the ring-opening reaction of styrene oxide (methanol solvent) presence and absence of visible light irradiation, out of which S-CDs under visible light irradiation afforded 98% conversion which confirmed its efficiency as an acid catalyst,

whereas other catalysts exhibited moderate to better conversion efficiency. Moreover, the catalyst can be easily retained just by filtration and for three consecutive runs, no change in its catalytic property was observed [132].

### Carbon dots for perfluoroalkylation

Prato et al., in 2019 reported utilization of N-doped carbon dots (N-CDs) for the photocatalytic perfluoroalkylation of organic moieties. Hence, the authors utilized N-CDs in triggering the photocatalytic

**Table 1** Various synthesis methodology and applications of carbon dots based materials

S. No	Material	Source of CDs	Synthesis method	Applications in organic synthesis	Reference
1	Pd@CDs	Clotted cream	Thermal carbonization	Suzuki and Heck coupling	[36]
2	Pd@CDs@Fe <sub>3</sub> O <sub>4</sub>	Citric acid and urea	Thermal treatment	Suzuki–Miyaura reaction	[49]
3	Pd@CDs@Fe <sub>3</sub> O <sub>4</sub>	Vanillin	Thermal treatment	Suzuki–Miyaura reaction	[50]
4	Pd@MgO@CDs	Urea and PEG 200	Thermal treatment	Suzuki–Miyaura reaction	[51]
5	Pd@CDs@Fe <sub>3</sub> O <sub>4</sub>	Glycerol and urea	Thermal treatment	Suzuki reaction and nitro group reduction	[52]
6	Pd–Ag@CDs	D-glucose	Microwave-assisted hydrothermal treatment	Suzuki–Miyaura reaction	[53]
7	HPU/Pd@r-CDs	Starch-based carbon nanodots	Green reduction	Suzuki reaction	[54]
8	Amine-terminated CDs	A mixture of citric acid and amine	Pyrolysis	Knoevenagel condensation	[72]
9	BPEI(Branched polyethylene imine)-CDs	Citric acid	Carbonization	Knoevenagel condensation	[73]
10	g-C <sub>3</sub> N <sub>4</sub> -Pd/CDs@Fe	Glycerol and urea	Hydrothermal treatment	Sonogashira reaction	[80]
11	Sulfated carbon dots (s-CDs)	Glucose	Carbonization	Aerobic C–C coupling reaction of benzylic hydrocarbons	[81]
12	Hyperbranched polyurethane supported Pd–Ag@CDs	D-glucose	Microwave-assisted hydrothermal treatment	<i>ipso</i> -hydroxylation of aryl boronic acid	[82]
13	CDs	Graphite rods	Electrochemical method	Oxidation of alcohols	[94]
14	CDs/TiO <sub>2</sub>	Graphite rods	Electrochemical method	Oxidation of alcohols	[95]
15	CDs/Bi <sub>2</sub> MoO <sub>6</sub> nanocomposite	Citric acid and ethylenediamine	Hydrothermal method	Oxidative coupling of amines, photooxidation of toluene, and cascade synthesis of benzimidazole and benzothiazole	[96]
16	Carboxyl functionalized CDs	Dextrose in oleic acid	Microwave irradiation	Photocatalytic C–H oxidation of benzylic hydrocarbons	[97]
17	Au/NCD/MgAl-LDH (layered double hydroxide)	A mixture of dicyandiamide and citric acid	Thermal treatment	Base-free oxidation of benzyl alcohols	[98]
18	Fe/CDs/MnO <sub>2</sub>	Glucose	Incineration	Controlled oxidation of benzyl alcohols	[99]
19	CDs@IL(1-aminopropyl-3-methyl-imidazolium chloride)/WO <sub>4</sub> <sup>2-</sup>	Citric acid	Hydrothermal treatment	Selective oxidation of alcohols	[100]
20	CDs@DDA(dodecyl amine)-IL(1-aminopropyl-3-methyl-imidazolium chloride)/WO <sub>4</sub> <sup>2-</sup>	Citric acid	Hydrothermal treatment	Selective oxidation of alcohols in water	[101]

Table 1 continued

S. No	Material	Source of CDs	Synthesis method	Applications in organic synthesis	Reference
21	CDs/Cu <sub>2</sub> O nanocomposite	Fructose	Thermal treatment	Oxidative coupling of benzylamines	[102]
22	Co(Single atomically anchored catalyst) @CDs	Vitamin B <sub>12</sub>	Pyrolysis	Photocatalytic oxidative coupling of benzylamines	[103]
23	Oxygen-rich CDs (O-CDs)	Fullerene	Modified Hummers' method	Selective oxidation of amines and alcohols	[104]
24	Amphiphilic CDs/IL	Citric acid	Hydrothermal treatment	Oxidative cleavage of cinnamic acid derivatives, multi-substituted alkenes, and coumarin-3-carboxylic acid derivatives	[105]
25	Fe(III)-CDs	Xylene	Sonication	Hydrogenation of olefins	[106]
26	Sulfur and nitrogen co-doped CDs/g-C <sub>3</sub> N <sub>4</sub> nanocomposites	p-aminobenzenesulfonic acid	Hydrothermal method	Photoreduction of 4-nitrophenol	[107]
27	CDs/ZnCdS nanowires	Pyrene	Hydrothermal condition	Photoreduction of 4-nitroaniline to p-phenylenediamine	[108]
28	CDs@Pd-SnS <sub>2</sub> nanocomposite	Sucrose	Hydrothermal treatment	Photoreduction of aromatic nitro compounds	[109]
29	N-doped CDs	Derived from 4 different citric acid	Hydrothermal and pyrolysis	Photocleavage of methylene-oxygen (CH <sub>2</sub> -O) bond	[110]
30	Pd@CDs@Fe/cyclodextrin nanosponges-biochar hybrid	Glycerol and urea	Thermal treatment	Hydrogenation of nitroarenes	[111]
31	CDs/ZnIn <sub>2</sub> S <sub>4</sub> nanocomposite	Citric acid	Thermolysis	Hydrogenation of nitrobenzene to aniline, azoxybenzene and azobenzene	[112]
32	CDs-Ionic liquid	Citric acid	Pyrolysis	Synthesis of 4H-Chromene derivatives	[113]
33	Sulfonated CDs	Coconut shell char	Pyrolysis	Synthesis of amidoalkyl naphthol	[114]
34	Carbon nanodots (CDs)	$\beta$ -carotene	Hydrothermal treatment	Synthesis of dihydro/spiro/glycol quinazolinones and aza-Michael adducts	[115]
35	Fe <sub>3</sub> O <sub>4</sub> -CDs nanocomposite	PEG-200	Microwave treatment	Synthesis of quinazolinones	[116]
36	Fe <sub>3</sub> O <sub>4</sub> @CDs@SO <sub>3</sub> H	Candle soot	Thermal treatment	Synthesis of hexahydroquinoline derivatives	[117]
37	Prussian blue/CDs	D-Fructose	Alkaline hydrolysis	Oxidative cyanation of tertiary amines to $\alpha$ -aminonitriles	[125]
38	Cu(I)-CDs	Ascorbic acid	Thermolysis	Huisgen-1,3-dipolar cycloaddition	[131]
39	S-CDs	Graphite rod	Electrochemical method	Ring-opening of epoxides	[132]
40	Nitrogen-doped carbon nanodots (N-CDs)	Arginine and ethylenediamine	Microwave-assisted hydrothermal synthesis	Photocatalytic perfluoroalkylation of organic compounds	[133]

fluoroalkylation of organic compounds 107 with the electron-rich center by perfluoroalkyl iodides 106 under the reaction condition as described in (Scheme 43) to give the corresponding fluoro

alkylated products 108 in high yield of 93% within 24 h of reaction time. Furthermore, the recyclability of catalysts has not been reported [133].

## Summary

Table 1 describes the overall summary of CDs prepared from different sources by different synthesis methods and their catalytic application in various organic reactions.

## Conclusion and future perspectives

Carbon dots are excellent candidates with their outstanding physicochemical properties which could be tailored with numerous materials like metal oxides, metals, polymers, etc., to form nanocomposites or nanohybrids. In this review, several literature methods have been reported with the use of these carbon dots supported materials in a variety of organic transformations like carbon–carbon bond formation, oxidation, reduction, hydrogenation, heterocyclic synthesis, multi-component synthesis, and simple organic conversions. Also, recent advancements of carbon dots to develop it as an amphiphilic catalyst have been reported here as a recent novelty in the chemistry of carbon dots. Whilst good progress has been achieved so far, there are still many unresolved constraints and openings to be explored. One of the key issues is determining the precise development procedures of CDs and, more particularly, the formation of their surface groups. Furthermore, despite repeated attempts, a detailed understanding of CDs framework in regard to reactivity, nature, and affordability of their functionalities is frequently lacking. Particularly, with this knowledge, the construction of innovative nanocatalytic techniques would be simplified, permitting their application to discover novel reactivities. In this regard, we anticipate the emergence of a spate of relevant organic reactions in the near future. Undoubtedly, carbon dots are extraordinary materials that will fix the existing challenges in the field of green and organic synthesis.

## References

- [1] Kang Z, Lee ST (2019) Carbon dots: advances in nanocarbon applications. *Nanoscale* 11:19214–19224. <https://doi.org/10.1039/c9nr05647e>
- [2] Yu H, Shang L, Bian T et al (2016) Nitrogen-doped porous carbon nanosheets templated from g-C<sub>3</sub>N<sub>4</sub> as metal-free electrocatalysts for efficient oxygen reduction reaction. *Adv Mater* 28:5080–5086. <https://doi.org/10.1002/adma.201600398>
- [3] Liu W, Li C, Ren Y et al (2016) Carbon dots: surface engineering and applications. *J Mater Chem B* 4:5772–5788. <https://doi.org/10.1039/c6tb00976j>
- [4] Filippini G, Prato M, Rosso C (2020) Carbon dots as nano-organocatalysts for synthetic applications. *ACS Catal* 10:8090–8105. <https://doi.org/10.1021/acscatal.0c01989>
- [5] Wang R, Lu KQ, Tang ZR, Xu YJ (2017) Recent progress in carbon quantum dots: synthesis, properties and applications in photocatalysis. *J Mater Chem A* 5:3717–3734. <https://doi.org/10.1039/c6ta08660h>
- [6] Das R, Bandyopadhyay R, Pramanik P (2018) Carbon quantum dots from natural resource: a review. *Mater Today Chem* 8:96–109. <https://doi.org/10.1016/j.mtchem.2018.03.003>
- [7] Li X, Rui M, Song J et al (2015) Carbon and graphene quantum dots for optoelectronic and energy devices: a review. *Adv Funct Mater* 25:4929–4947. <https://doi.org/10.1002/adfm.201501250>
- [8] Lim SY, Shen W, Gao Z (2015) Carbon quantum dots and their applications. *Chem Soc Rev* 44:362–381. <https://doi.org/10.1039/c4cs00269e>
- [9] Wang X, Cao L, Lu F et al (2009) Photoinduced electron transfers with carbon dots. *Chem Commun* 46(25):3774–3776. <https://doi.org/10.1039/b906252a>
- [10] Xia J, Di J, Li H et al (2016) Ionic liquid-induced strategy for carbon quantum dots/BiOX (X=Br, Cl) hybrid nanosheets with superior visible light-driven photocatalysis. *Appl Catal B Environ* 181:260–269. <https://doi.org/10.1016/j.apcatb.2015.07.035>
- [11] Di J, Xia J, Huang Y et al (2016) Constructing carbon quantum dots/Bi<sub>2</sub>SiO<sub>5</sub> ultrathin nanosheets with enhanced photocatalytic activity and mechanism investigation. *Chem Eng J* 302:334–343. <https://doi.org/10.1016/j.cej.2016.05.009>
- [12] Fang S, Xia Y, Lv K et al (2016) Effect of carbon-dots modification on the structure and photocatalytic activity of g-C<sub>3</sub>N<sub>4</sub>. *Appl Catal B Environ* 185:225–232. <https://doi.org/10.1016/j.apcatb.2015.12.025>
- [13] Hu S, Zhou Y, Xue C et al (2017) A solid reaction towards: in situ hybridization of carbon dots and conjugated polymers for enhanced light absorption and conversion. *Chem Commun* 53:9426–9429. <https://doi.org/10.1039/c7cc05526a>

- [14] Cao L, Sahu S, Anilkumar P et al (2011) Carbon nanoparticles as visible-light photocatalysts for efficient CO<sub>2</sub> conversion and beyond. *J Am Chem Soc* 133:4754–4757. <https://doi.org/10.1021/ja200804h>
- [15] Yu H, Zhao Y, Zhou C et al (2014) Carbon quantum dots/TiO<sub>2</sub> composites for efficient photocatalytic hydrogen evolution. *J Mater Chem A* 2:3344–3351. <https://doi.org/10.1039/c3ta14108j>
- [16] Liu J, Liu Y, Liu N et al (2015) Metal-free efficient photocatalyst for stable visible water splitting via a two-electron pathway. *Science* 347:970–974. <https://doi.org/10.1126/science.aaa3145>
- [17] Martindale BCM, Hutton GAM, Caputo CA, Reisner E (2015) Solar hydrogen production using carbon quantum dots and a molecular nickel catalyst. *J Am Chem Soc* 137:6018–6025. <https://doi.org/10.1021/jacs.5b01650>
- [18] Guo CX, Dong Y, Bin YH, Li CM (2013) Graphene quantum dots as a green sensitizer to functionalize ZnO nanowire arrays on F-doped SnO<sub>2</sub> glass for enhanced photoelectrochemical water splitting. *Adv Energ Mater* 3:997–1003. <https://doi.org/10.1002/aenm.201300171>
- [19] Chu KW, Lee SL, Chang CJ, Liu L (2019) Recent progress of carbon dot precursors and photocatalysis applications. *Polymers* 11(2):206. <https://doi.org/10.3390/polym11040689>
- [20] Sharma A, Das J (2019) Small molecules derived carbon dots: Synthesis and applications in sensing, catalysis, imaging, and biomedicine. *J Nanobiotechnology* 17:1–24. <https://doi.org/10.1186/s12951-019-0525-8>
- [21] Li H, Liu R, Kong W et al (2014) Carbon quantum dots with photo-generated proton property as efficient visible light controlled acid catalyst. *Nanoscale* 6:867–873. <https://doi.org/10.1039/c3nr03996j>
- [22] Phang SJ, Tan LL (2019) Recent advances in carbon quantum dot (CQD)-based two dimensional materials for photocatalytic applications. *Catal Sci Technol* 9:5882–5905. <https://doi.org/10.1039/c9cy01452g>
- [23] Zhang Z, Yi G, Li P et al (2020) A minireview on doped carbon dots for photocatalytic and electrocatalytic applications. *Nanoscale* 12:13899–13906. <https://doi.org/10.1039/d0nr03163a>
- [24] Cayuela A, Soriano ML, Carrillo-Carrión C, Valcárcel M (2016) Semiconductor and carbon-based fluorescent nanodots: the need for consistency. *Chem Commun* 52(7):1311–1326
- [25] Georgakilas V, Perman JA, Tucek J, Zboril R (2015) Broad family of carbon nanoallotropes: classification, chemistry, and applications of fullerenes, carbon dots, nanotubes, graphene, nanodiamonds, and combined superstructures. *Chem Rev* 115(11):4744–4822
- [26] Hutton GA, Martindale BC, Reisner E (2017) Carbon dots as photosensitisers for solar-driven catalysis. *Chem Soc Rev* 46(20):6111–6123
- [27] Jelinek R (2017) Carbon quantum dots. Carbon nanostructures. Springer International Publishing, Cham, pp 29–46. <https://doi.org/10.1007/978-3-319-43911-2>
- [28.] Gao J, Zhu M, Huang H, Liu Y, Kang Z (2017) Advances, challenges and promises of carbon dots. *Inorg Chem Front* 4(12):1963–1986
- [29] Miao X, Qu D, Yang D, Nie B, Zhao Y, Fan H, Sun Z (2018) Synthesis of carbon dots with multiple color emission by controlled graphitization and surface functionalization. *Adv Mater* 30(1):1704740
- [30] Arcudi F, Đorđević L, Prato M (2017) Rationally designed carbon nanodots towards pure white-light emission. *Angew Chem Int Ed* 56(15):4170–4173
- [31] Lu S, Xiao G, Sui L, Feng T, Yong X, Zhu S, Yang B (2017) Piezochromic carbon dots with two-photon fluorescence. *Angew Chem* 129(22):6283–6287
- [32] Mintz KJ, Zhou Y, Leblanc RM (2019) Recent development of carbon quantum dots regarding their optical properties, photoluminescence mechanism, and core structure. *Nanoscale* 11(11):4634–4652
- [33] Yan F, Sun Z, Zhang H, Sun X, Jiang Y, Bai Z (2019) The fluorescence mechanism of carbon dots, and methods for tuning their emission color: a review. *Microchim Acta* 186(8):1–37
- [34] Arcudi F, Đorđević L, Prato M (2016) Synthesis, separation, and characterization of small and highly fluorescent nitrogen-doped carbon nanodots. *Angew Chem* 128(6):2147–2152
- [35] Li X, Zhang S, Kulinich SA, Liu Y, Zeng H (2014) Engineering surface states of carbon dots to achieve controllable luminescence for solid-luminescent composites and sensitive Be<sup>2+</sup> detection. *Sci Rep* 4(1):1–8
- [36] Dey D, Bhattacharya T, Majumdar B, Mandani S et al (2013) Carbon dot reduced palladium nanoparticles as active catalysts for carbon-carbon bond formation. *Dalton Trans* 42:13821–13825. <https://doi.org/10.1039/C3DT51234G>
- [37] Pagliaro M, Pandarus V, Beland F, Ciriminna R, Palmisano G, Cara PD (2011) A new class of heterogeneous Pd catalysts for synthetic organic chemistry. *Catal Sci Technol* 1(5):736–739
- [38] Yabe Y, Sawama Y, Monguchi Y, Sajiki H (2014) New aspect of chemoselective hydrogenation utilizing heterogeneous palladium catalysts supported by nitrogen-and oxygen-containing macromolecules. *Catal Sci Technol* 4(2):260–271

- [39] Mora M, Jimenez-Sanchidrian C, Rafael Ruiz J (2012) Recent advances in the heterogeneous palladium-catalysed Suzuki cross-coupling reaction. *Curr Org Chem* 16(9):1128–1150
- [40] Yin L, Liebscher J (2007) Carbon– carbon coupling reactions catalyzed by heterogeneous palladium catalysts. *Chem Rev* 107(1):133–173
- [41] Pagliaro M, Pandarus V, Ciriminna R, Béland F, Demma Carà P (2012) Heterogeneous versus homogeneous palladium catalysts for cross-coupling reactions. *ChemCatChem* 4(4):432–445
- [42] Karimi B, Behzadnia H, Vali H (2014) Palladium on ionic liquid derived nanofibrillated mesoporous carbon: a recyclable catalyst for the ullmann homocoupling reactions of aryl halides in water. *ChemCatChem* 6(3):745–748
- [43] Polshettiwar V, Molnár Á (2007) Silica-supported Pd catalysts for Heck coupling reactions. *Tetrahedron* 30(63):6949–6976
- [44] Nehra P, Khungar B, Pericherla K, Sivasubramanian SC, Kumar A (2014) Imidazolium ionic liquid-tagged palladium complex: an efficient catalyst for the Heck and Suzuki reactions in aqueous media. *Green Chem* 16(9):4266–4271
- [45] Gong Y, Li M, Li H, Wang Y (2015) Graphitic carbon nitride polymers: promising catalysts or catalyst supports for heterogeneous oxidation and hydrogenation. *Green Chem* 17(2):715–736
- [46] Ghaderi A, Gholinejad M, Firouzabadi H (2016) Palladium deposited on naturally occurring supports as a powerful catalyst for carbon-carbon bond formation reactions. *Curr Org Chem* 20(4):327–348
- [47] Karimi B, Mansouri F, Mirzaei HM (2015) Recent applications of magnetically recoverable nanocatalysts in C-C and C-X coupling reactions. *ChemCatChem* 7(12):1736–1789
- [48] Veisi H, Gholami J, Ueda H, Mohammadi P, Noroozi M (2015) Magnetically palladium catalyst stabilized by diaminoglyoxime-functionalized magnetic Fe<sub>3</sub>O<sub>4</sub> nanoparticles as active and reusable catalyst for Suzuki coupling reactions. *J Mol Catal A Chem* 396:216–223
- [49] Gholinejad M, Seyedhamzeh M, Razeghi M et al (2016) Iron oxide nanoparticles modified with carbon quantum nanodots for the stabilization of palladium nanoparticles: an efficient catalyst for the Suzuki reaction in aqueous media under mild conditions. *ChemCatChem* 8:441–447. <https://doi.org/10.1002/cctc.201500925>
- [50] Gholinejad M, Najera C, Hamed F et al (2017) Green synthesis of carbon quantum dots from vanillin for modification of magnetite nanoparticles and formation of palladium nanoparticles: efficient catalyst for Suzuki reaction. *Tetrahedron* 73:5585–5592. <https://doi.org/10.1016/j.tet.2016.11.014>
- [51] Gholinejad M, Bahrami M, Nájera C (2017) A fluorescence active catalyst support comprising carbon quantum dots and magnesium oxide doping for stabilization of palladium nanoparticles: application as a recoverable catalyst for Suzuki reaction in water. *Mol Catal* 433:12–19. <https://doi.org/10.1016/j.mcat.2016.12.010>
- [52] Gholinejad M, Zareh F, Nájera C (2018) Nitro group reduction and Suzuki reaction catalysed by palladium supported on magnetic nanoparticles modified with carbon quantum dots generated from glycerol and urea. *Appl Organomet Chem* 32:1–14. <https://doi.org/10.1002/aoc.3984>
- [53] Bayan R, Karak N (2017) Photo-assisted synthesis of a Pd-Ag@CQD nanohybrid and its catalytic efficiency in promoting the Suzuki-Miyaura cross-coupling reaction under ligand-free and ambient conditions. *ACS Omega* 2:8868–8876. <https://doi.org/10.1021/acsomega.7b01504>
- [54] Duarah R, Karak N (2019) Hyperbranched polyurethane/palladium-reduced carbon dot nanocomposite: an efficient and reusable mesoporous catalyst for visible-light-driven C–C coupling reactions. *Ind Eng Chem Res* 58:16307–16319. <https://doi.org/10.1021/acs.iecr.9b01805>
- [55] Bigi F, Chesini L, Maggi R, Sartori G (1999) Montmorillonite KSF as an inorganic, water stable, and reusable catalyst for the Knoevenagel synthesis of coumarin-3-carboxylic acids. *J Org Chem* 64(3):1033–1035. <https://doi.org/10.1021/jo981794r>
- [56] Yu N, Aramini JM, Germann MW, Huang Z (2000) Reactions of salicylaldehydes with alkyl cyanoacetates on the surface of solid catalysts: syntheses of 4H-chromene derivatives. *Tetrahedron Lett* 41(36):6993–6996. [https://doi.org/10.1016/S0040-4039\(00\)01195-3](https://doi.org/10.1016/S0040-4039(00)01195-3)
- [57] Liang F, Pu Y-J, Kurata T, Kido J, Nishide H (2005) Synthesis and electroluminescent property of poly (p-phenylenevinylene)s bearing triarylamine pendants. *Polymer* 46(11):3767–3775. <https://doi.org/10.1016/j.polymer.2005.03.036>
- [58] Texier-Boullet F, Foucaud A (1982) Knoevenagel condensation catalysed by aluminium oxide. *Tetrahedron Lett* 23(47):4927–4928. [https://doi.org/10.1016/S0040-4039\(00\)85749-4](https://doi.org/10.1016/S0040-4039(00)85749-4)
- [59] Rao PS, Venkataratnam R (1991) Zinc chloride as a new catalyst for Knoevenagel condensation. *Tetrahedron Lett* 32(41):5821–5822. [https://doi.org/10.1016/S0040-4039\(00\)93564-0](https://doi.org/10.1016/S0040-4039(00)93564-0)
- [60] Bartoli G, Bosco M, Carlone A, Dalpozzo R, Galzerano P, Melchiorre P, Sambri L (2008) Magnesium perchlorate as

- efficient lewis acid for the Knoevenagel condensation between  $\beta$ -diketones and aldehydes. *Tetrahedron Lett* 49(16):2555–2557. <https://doi.org/10.1016/j.tetlet.2008.02.093>
- [61] Climent MJ, Corma A, Domínguez I, Iborra S, Sabater MJ, Sastre G (2007) Gem-diamines as highly active organocatalysts for carbon–carbon bond formation. *J Catal* 246(1):136–146. <https://doi.org/10.1016/j.jcat.2006.11.029>
- [62] Saravanamurugan S, Palanichamy M, Hartmann M, Murugesan V (2006) Knoevenagel condensation over  $\beta$  and Y zeolites in liquid phase under solvent free conditions. *Appl Catal A* 298:8–15. <https://doi.org/10.1016/j.apcata.2005.09.014>
- [63] Kubota Y, Nishizaki Y, Ikeya H, Saeki M, Hida T, Kawazu S, Yoshida M, Fujii H, Sugi Y (2004) Organic–silicate hybrid catalysts based on various defined structures for Knoevenagel condensation. *Microporous Mesoporous Mater* 70(1–3):135–149. <https://doi.org/10.1016/j.micromeso.2004.02.017>
- [64] Mukhopadhyay C, Ray S (2011) A new silica based substituted piperidine derivative catalyzed expeditious room temperature synthesis of homo and hetero bis-Knoevenagel condensation products. *Catal Commun* 12(15):1496–1502. <https://doi.org/10.1016/j.catcom.2011.05.033>
- [65] Varadwaj GBB, Rana S, Parida K (2013) Amine functionalized K10 montmorillonite: a solid acid–base catalyst for the Knoevenagel condensation reaction. *Dalton Trans* 42(14):5122–5129. <https://doi.org/10.1039/c3dt32495h>
- [66] Panchenko VN, Matrosova MM, Jeon J, Jun JW, Timofeeva MN, Jung SH (2014) Catalytic behavior of metal–organic frameworks in the Knoevenagel condensation reaction. *J Catal* 316:251–259. <https://doi.org/10.1016/j.jcat.2014.05.018>
- [67] Yang Y, Yao H-F, Xi F-G, Gao E-Q (2014) Amino-functionalized Zr (IV) metal–organic framework as bifunctional acid–base catalyst for Knoevenagel condensation. *J Mol Catal A* 390:198–205. <https://doi.org/10.1016/j.molcata.2014.04.002>
- [68] Tran UP, Le KK, Phan NT (2011) Expanding applications of metal–organic frameworks: zeolite imidazolate framework ZIF-8 as an efficient heterogeneous catalyst for the Knoevenagel reaction. *ACS Catal* 1(2):120–127. <https://doi.org/10.1021/cs1000625>
- [69] Nguyen LT, Le KK, Truong HX, Phan NT (2012) Metal–organic frameworks for catalysis: the Knoevenagel reaction using zeolite imidazolate framework ZIF-9 as an efficient heterogeneous catalyst. *Catal Sci Technol* 2(3):521–528. <https://doi.org/10.1039/c1cy00386k>
- [70] Xamena FL, Cirujano F, Corma A (2012) An unexpected bifunctional acid base catalysis in IRMOF-3 for Knoevenagel condensation reactions. *Microporous Mesoporous Mater* 157:112–117. <https://doi.org/10.1016/j.micromeso.2011.12.058>
- [71] Farzaneh F, Maleki MK, Rashtizadeh E (2017) Expedient catalytic access to Knoevenagel condensation using Sr<sub>3</sub>Al<sub>2</sub>O<sub>6</sub> nanocomposite in room temperature. *J Clust Sci* 28(6):3253–3263. <https://doi.org/10.1007/s10876-017-1288-8>
- [72] Pei X, Xiong D, Wang H et al (2018) Reversible phase transfer of carbon dots between an organic phase and aqueous solution triggered by CO<sub>2</sub>. *Angew Chemie* 130:3749–3753. <https://doi.org/10.1002/ange.201800037>
- [73] Farzaneh F, Aghabali S, Azarkamanzad Z (2020) Polyamine-functionalized carbon dots as active catalyst for Knoevenagel condensation reactions. *React Kinet Mech Catal* 130:1009–1025. <https://doi.org/10.1007/s11144-020-01826-4>
- [74] Bakherad M, Bahramian B, Jajarmi S (2014) A novel 1, 2, 4-triazine-functionalized polystyrene resin-supported Pd (II) complex: a copper-and solvent-free highly efficient catalyst for Sonogashira coupling reactions. *J Organomet Chem* 749:405–409
- [75] Roy S, Plenio H (2010) Sulfonated N-heterocyclic carbenes for Pd-catalyzed Sonogashira and Suzuki-Miyaura coupling in aqueous solvents. *Adv Synth Catal* 352(6):1014–1022
- [76] Hajipour AR, Shirdashtzade Z, Azizi G (2014) Copper-and phosphine-free Sonogashira coupling reaction catalyzed by silica-(acac)-supported palladium nanoparticles in water. *Appl Organomet Chem* 28(9):696–698
- [77] Thorwirth R, Stolle A, Ondruschka B (2010) Fast copper-, ligand-and solvent-free Sonogashira coupling in a ball mill. *Green Chem* 12(6):985–991
- [78] Shunmughanathan M, Puthiaraj P, Pitchumani K (2015) Melamine-based microporous network polymer supported palladium nanoparticles: a stable and efficient catalyst for the sonogashira coupling reaction in water. *ChemCatChem* 7(4):666–673
- [79] Le X, Dong Z, Liu Y, Jin Z, Huy TD, Le M, Ma J (2014) Palladium nanoparticles immobilized on core–shell magnetic fibers as a highly efficient and recyclable heterogeneous catalyst for the reduction of 4-nitrophenol and Suzuki coupling reactions. *J Mater Chem A* 2(46):19696–19706
- [80] Mohammadi L, Heravi MM, Sadjadi S, Malmir M (2019) Hybrid of graphitic carbon nitride and palladated magnetic carbon dot: an efficient catalyst for coupling reaction. *ChemistrySelect* 4:13404–13411. <https://doi.org/10.1002/slct.201903078>
- [81] Sarma D, Majumdar B, Sarma TK (2019) Visible-light induced enhancement in the multi-catalytic activity of sulfated carbon dots for aerobic carbon-carbon bond

- formation. *Green Chem* 21:6717–6726. <https://doi.org/10.1039/c9gc02658d>
- [82] Bayan R, Karak N (2018) Hyperbranched polyurethane-supported Pd-Ag@CQD nanocomposite: a high performing heterogeneous catalyst. *ChemistrySelect* 3:11210–11218. <https://doi.org/10.1002/slct.201802403>
- [83] Mallat T, Baiker A (2004) Oxidation of alcohols with molecular oxygen on solid catalysts. *Chem Rev* 104(6):3037–3058
- [84] Paraskevopoulou P, Psaroudakis N, Koinis S, Stavropoulos P, Mertis K (2005) Catalytic selective oxidation of benzyl alcohols to aldehydes with rhenium complexes. *J Mol Catal A Chem* 240(1–2):27–32
- [85] Li G, Enache DI, Edwards J, Carley AF, Knight DW, Hutchings GJ (2006) Solvent-free oxidation of benzyl alcohol with oxygen using zeolite-supported Au and Au–Pd catalysts. *Catal Lett* 110(1):7–13
- [86] Dijksman A, Marino-Gonzalez A, Mairata I, Payeras A, Arends IW, Sheldon RA (2001) Efficient and selective aerobic oxidation of alcohols into aldehydes and ketones using ruthenium/TEMPO as the catalytic system. *J Am Chem Soc* 123(28):6826–6833
- [87] Yamamoto R, Sawayama YS, Shibahara H, Ichihashi Y, Nishiyama S, Tsuruya S (2005) Promoted partial oxidation activity of supported Ag catalysts in the gas-phase catalytic oxidation of benzyl alcohol. *J Catal* 234(2):308–317
- [88] Zhan G, Huang J, Du M, Sun D, Abdul-Rauf I, Lin W, Li Q (2012) Liquid phase oxidation of benzyl alcohol to benzaldehyde with novel uncalcined bioreduction Au catalysts: high activity and durability. *Chem Eng J* 187:232–238
- [89] Choudhary VR, Dhar A, Jana P, Jha R, Uphade BS (2005) A green process for chlorine-free benzaldehyde from the solvent-free oxidation of benzyl alcohol with molecular oxygen over a supported nano-size gold catalyst. *Green Chem* 7(11):768–770
- [90] Chen Y, Lim H, Tang Q, Gao Y, Sun T, Yan Q, Yang Y (2010) Solvent-free aerobic oxidation of benzyl alcohol over Pd monometallic and Au–Pd bimetallic catalysts supported on SBA-16 mesoporous molecular sieves. *Appl Catal A* 380(1–2):55–65
- [91] Villa A, Wang D, Dimitratos N, Su D, Trevisan V, Prati L (2010) Pd on carbon nanotubes for liquid phase alcohol oxidation. *Catal Today* 150(1–2):8–15
- [92] Fu X, Yu H, Peng F, Wang H, Qian Y (2007) Facile preparation of RuO<sub>2</sub>/CNT catalyst by a homogenous oxidation precipitation method and its catalytic performance. *Appl Catal A* 321(2):190–197
- [93] Fu X, Feng J, Wang H, Ng KM (2010) Fast synthesis and formation mechanism of  $\gamma$ -MnO<sub>2</sub> hollow nanospheres for aerobic oxidation of alcohols. *Mater Res Bull* 45(9):1218–1223
- [94] Zhang X, Fu X, Zhang Y et al (2016) Transition metal-free carbon quantum dots for selective liquid phase oxidation of alcohols using water as an only solvent. *Catal Lett* 146:945–950. <https://doi.org/10.1007/s10562-016-1714-9>
- [95] Ren P, Fu X, Zhang Y (2017) Carbon quantum dots-TiO<sub>2</sub> nanocomposites with enhanced catalytic activities for selective liquid phase oxidation of alcohols. *Catal Lett* 147:1679–1685. <https://doi.org/10.1007/s10562-017-2065-x>
- [96] Samanta S, Khilari S, Srivastava R (2018) Stimulating the visible-light catalytic activity of Bi<sub>2</sub>MoO<sub>6</sub> nanoplates by embedding carbon dots for the efficient oxidation, cascade reaction, and photoelectrochemical O<sub>2</sub> evolution. *ACS Appl Nano Mater* 1:426–441. <https://doi.org/10.1021/acsnm.7b00282>
- [97] Sarma D, Majumdar B, Sarma TK (2018) Carboxyl-functionalized carbon dots as competent visible light photocatalysts for aerobic oxygenation of alkyl benzenes: role of surface functionality. *ACS Sustain Chem Eng* 6:16573–16585. <https://doi.org/10.1021/acssuschemeng.8b03811>
- [98] Guo Y, Fan L, Liu M et al (2020) Nitrogen-doped carbon quantum dots-decorated Mg–Al layered double hydroxide-supported gold nanocatalysts for efficient base-free oxidation of benzyl alcohol. *Ind Eng Chem Res* 59:636–646. <https://doi.org/10.1021/acs.iecr.9b04296>
- [99] Prathibha E, Rangasamy R, Sridhar A, Lakshmi K (2020) Synthesis and characterization of Fe<sub>3</sub>O<sub>4</sub>/carbon dot supported MnO<sub>2</sub> nanoparticles for the controlled oxidation of benzyl alcohols. *ChemistrySelect* 5:988–993. <https://doi.org/10.1002/slct.201903706>
- [100] Mohammadi M, Khazaei A, Rezaei A et al (2019) Ionic-liquid-modified carbon quantum dots as a support for the immobilization of tungstate ions (WO<sub>4</sub><sup>2-</sup>): heterogeneous nanocatalysts for the oxidation of alcohols in water. *ACS Sustain Chem Eng* 7:5283–5291. <https://doi.org/10.1021/acssuschemeng.8b06279>
- [101] Mohammadi M, Rezaei A, Khazaei A et al (2019) Targeted development of sustainable green catalysts for oxidation of alcohols via tungstate-decorated multifunctional amphiphilic carbon quantum dots. *ACS Appl Mater Interfaces* 11:33194–33206. <https://doi.org/10.1021/acsnm.9b07961>
- [102] Kumar A, Hamdi A, Coffinier Y et al (2018) Visible light assisted oxidative coupling of benzylamines using heterostructured nanocomposite photocatalyst. *J Photochem Photobiol A* 356:457–463. <https://doi.org/10.1016/j.jphotochem.2018.01.033>



- [103] Wang Q, Li J, Tu X et al (2020) Single atomically anchored cobalt on carbon quantum dots as efficient photocatalysts for visible light-promoted oxidation reactions. *Chem Mater* 32:734–743. <https://doi.org/10.1021/acs.chemmater.9b03708>
- [104] Ye J, Ni K, Liu J et al (2018) Oxygen-rich carbon quantum dots as catalysts for selective oxidation of amines and alcohols. *ChemCatChem* 10:259–265. <https://doi.org/10.1002/cctc.201701148>
- [105] Hadian-Dehkordi L, Rezaei A, Ramazani A et al (2020) Amphiphilic carbon quantum dots as a bridge to a pseudohomogeneous catalyst for selective oxidative cracking of alkenes to aldehydes: a nonmetallic oxidation system. *ACS Appl Mater Interfaces* 12:31360–31371. <https://doi.org/10.1021/acsami.0c05025>
- [106] Bourlinos AB, Rathi AK, Gawande MB et al (2017) Fe(III)-functionalized carbon dots—Highly efficient photoluminescence redox catalyst for hydrogenations of olefins and decomposition of hydrogen peroxide. *Appl Mater Today* 7:179–184. <https://doi.org/10.1016/j.apmt.2017.03.002>
- [107] Chang Q, Yang S, Li L et al (2018) Loading sulfur and nitrogen co-doped carbon dots onto g-C<sub>3</sub>N<sub>4</sub> nanosheets for an efficient photocatalytic reduction of 4-nitrophenol. *Dalt Trans* 47:6435–6443. <https://doi.org/10.1039/c8dt00735g>
- [108] Chai YY, Qu DP, Ma DK et al (2018) Carbon quantum dots/Zn<sup>2+</sup> ions doped-CdS nanowires with enhanced photocatalytic activity for reduction of 4-nitroaniline to p-phenylenediamine. *Appl Surf Sci* 450:1–8. <https://doi.org/10.1016/j.apsusc.2018.04.121>
- [109] Liu M, Wang R, Liu B et al (2019) Carbon quantum dots @ Pd-SnS<sub>2</sub> nanocomposite: the role of CQDs @ Pd nanoclusters in enhancing photocatalytic reduction of aromatic nitro compounds. *J Coll Interface Sci* 555:423–430. <https://doi.org/10.1016/j.jcis.2019.08.002>
- [110] Cailotto S, Negrato M, Daniele S et al (2020) Carbon dots as photocatalysts for organic synthesis: metal-free methylene-oxygen-bond photocleavage. *Green Chem* 22:1145–1149. <https://doi.org/10.1039/c9gc03811f>
- [111] Sadjadi S, Heravi MM, Mohammadi L, Malmir M (2019) Pd@magnetic carbon dot immobilized on the cyclodextrin nanosponges - biochar hybrid as an efficient hydrogenation catalyst. *ChemistrySelect* 4:7300–7307. <https://doi.org/10.1002/slct.201901451>
- [112] Wang B, Deng Z, Li Z (2020) Efficient chemoselective hydrogenation of nitrobenzene to aniline, azoxybenzene and azobenzene over CQDs/ZnIn<sub>2</sub>S<sub>4</sub> nanocomposites under visible light. *J Catal* 389:241–246. <https://doi.org/10.1016/j.jcat.2020.05.041>
- [113] Mayank SA, Kaur N et al (2017) A carbon quantum dot-encapsulated micellar reactor for the synthesis of chromene derivatives in water. *Mol Catal* 439:100–107. <https://doi.org/10.1016/j.mcat.2017.06.032>
- [114] Narayanan DP, Cherikallinmel SK, Sankaran S, Narayanan BN (2018) Functionalized carbon dot adorned coconut shell char derived green catalysts for the rapid synthesis of amidoalkyl naphthols. *J Coll Interface Sci* 520:70–80. <https://doi.org/10.1016/j.jcis.2018.02.077>
- [115] Majumdar B, Mandani S, Bhattacharya T et al (2017) Probing carbocatalytic activity of carbon nanodots for the synthesis of biologically active dihydro/spiro/glyco quinazolinones and aza-michael adducts. *J Org Chem* 82:2097–2106. <https://doi.org/10.1021/acs.joc.6b02914>
- [116] Majumdar B, Sarma D, Jain S, Sarma TK (2018) One-pot magnetic iron oxide-carbon nanodot composite-catalyzed cyclooxidative aqueous tandem synthesis of quinazolinones in the presence of tert-butyl hydroperoxide. *ACS Omega* 3:13711–13719. <https://doi.org/10.1021/acsomega.8b01794>
- [117] Sarmasti N, Khazaei A, Yousefi Seyf J (2019) High density sulfonated magnetic carbon quantum dots as a photo enhanced, photo-induced proton generation, and photo switchable solid acid catalyst for room temperature one-pot reaction. *Res Chem Intermed* 45:3929–3942. <https://doi.org/10.1007/s11164-019-03829-w>
- [118] Shi L, Xia W (2012) Photoredox functionalization of C-H bonds adjacent to a nitrogen atom. *Chem Soc Rev* 41(23):7687–7697
- [119] To WP, Liu Y, Lau TC, Che CM (2013) A robust palladium (II)–porphyrin complex as catalyst for visible light induced oxidative C-H functionalization. *Chem Eur J* 19(18):5654–5664
- [120] North M (2004) Oxidative synthesis of  $\alpha$ -amino nitriles from tertiary amines. *Angew Chem Int Ed* 43(32):4126–4128
- [121] Guo S, Qian B, Xie Y, Xia C, Huang H (2011) Copper-catalyzed oxidative amination of benzoxazoles via C–H and C–N bond activation: a new strategy for using tertiary amines as nitrogen group sources. *Org Lett* 13(3):522–525
- [122] Enders D, Shilvock JP (2000) Some recent applications of  $\alpha$ -amino nitrile chemistry. *Chem Soc Rev* 29(5):359–373
- [123] Rueping M, Zhu S, Koenigs RM (2011) Visible-light photoredox catalyzed oxidative Strecker reaction. *Chem Commun* 47(47):12709–12711
- [124] Lalevée J, Peter M, Dumur F, Gigmes D, Blanchard N, Tehfe MA, Fouassier JP (2011) Subtle ligand effects in oxidative photocatalysis with iridium complexes: application to photopolymerization. *Chem Eur J* 17(52):15027–15031

- [125] Maaoui H, Kumar P, Kumar A, Pan GH et al (2016) A Prussian blue/carbon dot nanocomposite as an efficient visible light active photocatalyst for C-H activation of amines. *Photochem Photobiol Sci* 15:1282–1288. <https://doi.org/10.1039/C6PP00203J>
- [126] Kolb HC, Sharpless KB (2003) The growing impact of click chemistry on drug discovery. *Drug Discov Today* 8(24):1128–1137
- [127] Rostovtsev VV, Green LG, Fokin VV, Sharpless KB (2002) A stepwise Huisgen cycloaddition process: copper (I)-catalyzed regioselective “ligation” of azides and terminal alkynes. *Angew Chem* 114(14):2708–2711
- [128] Tornøe CW, Christensen C, Meldal M (2002) Peptidotriazoles on solid phase: [1, 2, 3]-triazoles by regiospecific copper (I)-catalyzed 1, 3-dipolar cycloadditions of terminal alkynes to azides. *J Org Chem* 67(9):3057–3064
- [129] Soriano del Amo D, Wang W, Jiang H, Besanceney C, Yan AC, Levy M, Wu P (2010) Biocompatible copper (I) catalysts for in vivo imaging of glycans. *J Am Chem Soc* 132(47):16893–16899
- [130] Bear JC, Hollingsworth N, McNaughton PD, Mayes AG, Ward MB, Nann T, Parkin IP (2014) Copper-doped CdSe/ZnS quantum dots: controllable photoactivated copper (I) cation storage and release vectors for catalysis. *Angew Chem Int Ed* 53(6):1598–1601
- [131] Liu ZX, Bin CB, Liu ML et al (2017) Cu(I)-doped carbon quantum dots with zigzag edge structures for highly efficient catalysis of azide-alkyne cycloadditions. *Green Chem* 19:1494–1498. <https://doi.org/10.1039/c6gc03288e>
- [132] Li H, Sun C, Ali M et al (2015) Sulfated carbon quantum dots as efficient visible-light switchable acid catalysts for room-temperature ring-opening reactions. *Angew Chemie Int Ed* 54:8420–8424. <https://doi.org/10.1002/anie.201501698>
- [133] Rosso C, Filippini G, Prato M (2019) Use of nitrogen-doped carbon nanodots for the photocatalytic fluoroalkylation of organic compounds. *Chem Eur J* 25:16032–16036. <https://doi.org/10.1002/chem.201903433>

**Publisher's Note** Springer Nature remains neutral with regard to jurisdictional claims in published maps and institutional affiliations.